



Impact of urbanization on gas-phase pollutant concentrations: a regional scale, model based analysis of the contributing factors

Peter Huszar¹, Jan Karlický¹, Lukáš Bartík¹, Marina Liaskoni¹, Alvaro Patricio Prieto Perez¹, and Kateřina Šindelářová¹

¹Department of Atmospheric Physics, Faculty of Mathematics and Physics, Charles University, Prague, V Holešovičkách 2, 18000, Prague 8, Czech Republic

Correspondence: P. Huszar (peter.huszar@mff.cuni.cz)

Abstract. Urbanization or rural-urban transformation (RUT) represents one of the most important transformations of land-use. To account for the impact of such process on air-quality, multiple aspects of how this transformation impacts the air has to be accounted for. Here we present a numerical model (regional climate models RegCM and WRF coupled to chemistry transport model CAMx) based study for present day conditions (2015-2016) focusing on a range of central European cities and quantify the individual and combined impact of four potential contributors. Apart from the two most studied impacts, i.e. the urban emissions and the urban canopy meteorological forcing (UCMF, i.e. the impact of modified meteorological conditions) we focus also on two less studied contributors to RUT: the impact of modified dry-deposition due to transformed landuse and the impact of modified biogenic emissions due to urbanization induced vegetation modifications and changes in meteorological conditions affecting these emissions. To quantify each of these RUT components, we performed a series of simulations with CAMx driven with both RegCM and WRF where each effect was added to the simulations one-by-one while we focused on gas-phase key pollutants: nitrogen and sulfur dioxide (NO₂ and SO₂) and ozone (O₃).

The validation of the results using surface observations showed an acceptable match between the modelled and observed annual cycles of monthly pollutant concentrations for NO₂ and O₃ while some discrepancies in the shape of the annual cycle were identified for some of the cities for SO₂ pointing to incorrect representation of the annual emission cycle in the emissions model used.

We showed on an ensemble 19 European cities that the most important contributors to the impact of RUT are the urban emissions themselves, resulting in increases concentrations for nitrogen dioxide (by 5-7 ppbv on average) and sulfur dioxide (by about 0.5-1 ppbv) and decreases for ozone (by about -2 ppbv) and the urban canopy meteorological forcing resulting in decreases of primary pollutants (by about 2 ppbv for NO₂ and 0.2 ppbv for SO₂) and increases of those of ozone (by about 2 ppbv). These are the two major drivers of urban air pollution and our results showed that they have to be accounted for simultaneously as the impact of urban emissions without considering UCMF can lead to overestimation of the emission impact. Additionally, we quantified two weaker contributors: the effect of modified landuse on dry-deposition and the effect of modified biogenic emissions. Due to modified dry-deposition summer (winter) NO₂ increases (decreases) by 0.05(0.02) ppbv while almost no average effect for SO₂ in summer and a 0.04 ppbv decrease in winter is modelled. The impact on ozone is much stronger and reaches a 1.5 ppbv increase on average. Due to modified biogenic emissions, negligible effect on SO₂ and



winter NO_2 is modelled, while for summer NO_2 , and increase by about 0.01 ppbv is calculated. For ozone, we found a much larger decreases between 0.5-1 ppbv.

In summary, when analyzing the overall impact of urbanization on air-pollution for ozone, all four components has to be accounted for while for primary pollutants (i.e. NO_2 and SO_2), the two minor contributors can be neglected.

30 1 Introduction

Urbanization represents one of the most important transformations of land-use turning the natural surface into an artificial one. While urban areas represent only less than a percent of the total Earth surface (Gao et al., 2020), already more than half of the earth's population live in cities (UN, 2018) and this transformation, which is often called rural-urban transformation (RUT) is still an ongoing process. It is expected that in the upcoming decades, 60% of the population will live in urban areas, making
35 the research focusing their environmental effects more and more crucial.

It has been known that urban areas affect predominantly the atmospheric environment (Folberth et al., 2015) and they act via two primary intrusions that urbanization represents within the natural environment: i) it is the introduction of urban land-surface replacing rural one causing significant modifications of the meteorological conditions (Oke et al., 2017) and climate (Huszar et al., 2014; Zhao et al., 2017), and ii) the introduction of a massive emissions source of anthropogenic pollutants
40 perturbing not only local but also regional and global air composition (Lawrence et al., 2007; Timothy and Lawrence, 2009; Im and Kanakidou, 2012; Huszar et al., 2016a).

As for the air-quality of urban areas and those surrounding large cities, it is clear that the main driver affecting the concentrations are the local urban emissions. Indeed, many studies looked on the perturbation of the atmospheric composition due to solely the urban emissions over different scales. E.g. Lawrence et al. (2007), Butler and Lawrence (2009) or Stock et al.
45 (2013) investigated the global impact of emissions from megacities, while on regional scales many studies focused on large agglomerations in Europe, like Athens, Istanbul, London or Paris (e.g. Im et al., 2011a, b; Im and Kanakidou, 2012; Finardi et al., 2014; Skyllakou et al., 2014; Markakis et al., 2015; Hodneborg et al., 2011; Huszar et al., 2016a; Hood et al., 2018) or on large eastern Asian pollution hot-spots (Guttikunda et al., 2003, 2005; Tie et al., 2013). There is further a general consensus in these studies, that although air pollution in cities is determined mainly by the local sources, significant fraction of the total
50 concentration is associated to rural sources or to sources from other cities (Panagi et al., 2020; Thunis et al., 2021; Huszar et al., 2021).

Urbanization however influences the final air pollution other ways too. One of the most studied aspect of RUT is the modulation of the pollutant concentration due to the meteorological forcing represented by the urban canopy which includes effects like higher temperatures (urban heat island, UHI) (Oke, 1982; Oke et al., 2017; Karlický et al., 2018; Karlický et al., 2020; Sokhi et al., 2022), lower wind-speeds (Jacobson et al., 2015; Zha et al., 2019) or elevated boundary layer height along with enhanced vertical eddy diffusion Ren et al. (2019); Huszar et al. (2020a); Wang et al. (2021b). Huszar et al. (2020a) introduced the term urban canopy meteorological forcing (UCMF) which represents the forcing that the land-surface modified by the RUT represents on the physical state of the air above via perturbed exchange of momentum, heat, radiation and moisture. UCMF



has well pronounced impact on air-quality modifying the transport, chemical transformation and deposition of air pollutants. Indeed, Ulpiani (2021) argued that the urban pollution has to be studied in connection with the UHI and other related effects. Many other studies looked at impact of UCMF on air-quality and found that the most important parameters in this regard are temperature, turbulence and wind (Struzewska and Kaminski, 2012; Liao et al., 2014; Kim et al., 2015; Zhu et al., 2017; Zhong et al., 2018; Li et al., 2019; Huszar et al., 2014, 2018a, 2020b) while moisture effects were rather minor (Huszar et al., 2018b). These studies found, that these changes led to near-surface decrease of primary pollutant concentrations while in case of secondary pollutants (e.g. ozone) increases are encountered either on the surface or at higher levels (Huszar et al., 2018a; Janssen et al., 2017; Yim et al., 2019; Li et al., 2019; Kim et al., 2021; Kang et al., 2022). In other words, besides the urban emission input, UCMF is another factor that contributes to the final urban pollution within the overall process of RUT (Huszar et al., 2021).

Moreover, during urbanization the land-use is modified from rural (or natural like forest/grassland etc.) to “urban” one which itself introduces a forcing via a further pathway: in contrary to wet-deposition, dry deposition velocities (DV) greatly depend on the land-use type which determines the resistance of the surface and canopy layer (Zhang et al., 2003; Cherin et al., 2015; Hardacre et al., 2021). In urban environments, vegetation is greatly reduced (expressed for example in term of the leaf-area-index LAI reduction). As plants represent a major sink for many gaseous air pollutants (via stomatal uptake), it is clear that over urban areas, this sink is missing or is strongly reduced. For example, based on the later study, over urban land-surface the typical DVs of nitrogen dioxide (NO_2) and ozone (O_3) are about half of that above agricultural land like crop (as typical rural land-surface type). McDonald-Buller et al. (2001) also showed that ozone and NO_2 is greater in a photochemical model if the landuse information supplied contains higher fraction of urban landuse type. In general it seems that besides other effects, urbanization leads to increased ozone concentrations due to reduced deposition values too (Song et al., 2008; Tao et al., 2015) while dry-deposition itself is an important factor determining ozone pollution (Galmarini et al., 2021). Recently, Hardacre et al. (2021) showed strong dependence of sulfur dioxide (SO_2) concentrations on dry-deposition depending on the surface type. It is thus clear, that the final air-pollution caused by urbanization has another component represented by the modified dry-deposition uptake potential of urban land-surface compared to rural/natural one.

Finally, vegetation does not act only as a sink of pollutants via dry-deposition by it also emits large amounts of biogenic hydrocarbons (biogenic volatile organic compounds; BVOC; Kesselmeier et al. (1999)). Due to their reactivity and potential to form peroxy-radicals, they contribute to the formation of tropospheric ozone (Situ et al., 2013; Tagaris et al., 2014). As mentioned already above, during urbanization, the vegetation is strongly reduced which will result in a decrease of BVOC emissions. Song et al. (2008) for example showed up to 10% reductions due to urbanization in Texas. As urban areas are usually VOC-limited environment, reduced BVOC emissions is expected to lead to reduced ozone concentrations (Song et al., 2008).

The urbanization induced BVOC emission modifications have a further sub-component acting via the modified meteorological conditions in cities. Indeed, urban temperatures are higher than rural ones and there is an indication that urban cloudiness, at least for European cities is slightly reduced too (Karlický et al., 2020). These effects have direct impact on the biochemistry of plants and thus on the amount of emitted BVOC as higher temperatures and more solar radiation promote these emissions



(Guenther et al., 2006). This means that due to urbanization, BVOC emissions are suppressed by reducing the vegetation frac-
95 tion, however, more favorable weather conditions act in opposite way making these effects counteracting. Although there is an
indication that the former (vegetation) effect is dominant (Li et al., 2019).

In summary, urbanization substantially affects air-quality while the final pollutant concentration levels are a result of multiple
impacts that add to the background (i.e. that without urbanization) air pollution:

1. The effect of urban emissions (“DEMIS”)
- 100 2. The effect of the urban canopy meteorological forcing (UCMF) on species transport and chemistry (“DMET”)
3. The effect of modified dry-deposition associated with modified land-cover (“DLU_D”)
4. The effect of modified emissions of biogenic volatile compounds (BVOC) due to modified land-cover (i) and meteorol-
ogy (ii) (“DBVOC”).

As seen above, many studies looked at the total impact of urbanization or at some of the individual components listed.
105 However, they did not systematically analyze the impact of each component. Here we propose a novel study to uncover the
contribution of each of these urbanization related impacts (i.e. “DEMIS”, “DMET”, “DLU_D” and “DBVOC”) as well as
the total impact (“DTOT”) over regional scale on the present day final air pollution levels using coupled regional climate
and chemistry transport models. To reduce the uncertainty of the results caused by the different geographical and climatic
conditions of cities, we perform our analysis for a large ensemble of cities in central Europe, 19 cities in total. Although, a
110 similar estimate across several urban areas was made in Huszar et al. (2016a), they focused only on the effect of emissions
only (which corresponds to “DEMIS” in our study) while none of other effects (UCMF, effect of landuse on dry-deposition and
effect of modified BVOC) was considered. The study will focus on key gas-phase pollutants NO_2 , O_3 and SO_2 . NO_2 is one
of the most important primary pollutants in urban environment responsible for reduced air-quality and being a precursor for
secondary pollutants like ozone or inorganic fine aerosol (Im and Kanakidou, 2012; Stock et al., 2013; Mertens et al., 2020).
115 Ozone is formed in urban plumes when NO_x and VOCs mix together promoted by solar radiation (Xue et al., 2014). Finally,
sulfur dioxide – a pollutant originating mainly from fossil fuel combustion in energy production (Guttikunda et al., 2003) –
has although undergone significant reduction in European cities during the last decades, it remains of concern, especially in
eastern European countries (e.g. in Poland; (EEA, 2019)).

The study is structured as follows: after the Introduction, the experimental tools (models), their configuration and the data
120 used are presented. Next, the experiments performed are presented followed by the Result section and finally, these are dis-
cussed and conclusions are drawn.



2 Methodology

2.1 Models used

The study is based on numerical experiments carried out using regional climate models (RCM) coupled to chemistry transport models (CTM). To describe the regional climate, two regional climate model as meteorological driver are used: RegCM version 4.7 and WRF version 4.0.3. Chemistry was resolved with the chemical transport model (CTM) CAMx in version 7.10. The decision behind choosing two regional meteorological drivers is to achieve, at least to some degree, more robust results given the fact that the modelled meteorological conditions over cities greatly impacts the chemical concentrations (Ďoubalová et al., 2020; Huszar et al., 2018b).

As the models used and the parameterizations applied are almost identical to those in Huszar et al. (2021), here we list the most important details. RegCM4.7 is a regional scale climate model with both hydrostatic and non-hydrostatic dynamics (Giorgi et al., 2012). The schemes adopted are: Tiedtke scheme (Tiedtke et al., 1989) for convection, Holtslag scheme (HOL; Holtslag et al., 1990) for PBL parameterization and the 5-class WSM5 moisture scheme (Hong et al., 2004) for microphysics. The CLMU urban canopy module implemented in the Community Land Model (CLM) version 4.5 (Oleson et al., 2008, 2010, 2013) land-surface scheme was used to resolve the urban scale meteorological phenomena while the traditional canyon geometry approach is implemented (Oke et al., 2017).

WRF (Weather Research and Forecasting) model is a regional weather prediction and climate model with detailed description provided by Skamarock et al. (2019). In our modelling setup, the Grell 3D convection scheme (Grell, 1993), the BouLac PBL scheme (Bougeault and Lacarrère, 1989), and the Purdue Lin scheme (Chen and Sun, 2002, PLIN;) for microphysics were used. The urban canopy meteorological effects were resolved using the Single-Layer Urban Canopy Model (SLUCM; (Kusaka et al., 2001)).

For the chemistry simulations the chemistry transport model CAMx version 7.10 (ENVIRON, 2020) was used (i.e. we used the most up-to-date version for CAMx available). CAMx is an Eulerian photochemical CTM implementing multiple gas phase chemistry schemes (Carbon Bond 5 and 6, SAPRC07TC etc.) with the Carbon Bond 6 revision 5 (CB6r5) scheme used in this study. CB6r5 includes updates to chemical reaction data from IUPAC (IUPAC, 2019) and NASA (Burkholder et al., 2019) for inorganic and simple organic species important for the formation of ozone. To complete the atmospheric chemistry with aerosol physics, static two mode approach was considered. The ISORROPIA thermodynamic equilibrium model (Nenes and Pandis, 1998) was invoked for the secondary inorganic aerosol formation. Secondary organic aerosol (SOA) were partitioned from their gas-phase precursors using the SOAP equilibrium scheme (Strader et al., 1999). For wet and dry deposition, the Seinfeld and Pandis (1998) and Zhang et al. (2003) methods were used, respectively.

Meteorological preprocessor is used to convert the RegCM and WRF meteorological data into model-ready driving data for CAMx: for the WRF, it was the wrfcamx preprocessor which is provided along with the CAMx code <http://www.camx.com/download/support-software.aspx> while for RegCM, the RegCM2CAMx interface was applied (Huszar et al., 2012) was applied. The vertical eddy diffusion coefficients (K_v) are diagnosed from the available meteorological data on RegCM and WRF output using the CMAQ diagnostic approach (Byun, 1999). Coupling between CAMx and the driving models is offline,



which implies that no feedbacks of the pollutant concentrations on WRF/RegCM radiation and microphysical processes were considered. Indeed, Huszar et al. (2016b) showed that their long-term effect is rather small which justified this choice.

2.2 Model setup and data

Model simulations were performed over identical domains (parent and nested ones) and for identical period as in Huszar et al. (2021), i.e. years 2015-2016 with 9 km, 3 km and 1 km horizontal resolution centered over the Czech capital, Prague (50.075° N, 14.44° E; Lambert Conic Conformal projection). In vertical, the model grid has 40 layers in both meteorological driving models. The thickness of the lowermost layer is about 30 m and the top of the model's atmosphere reaches 5 hPa (about 36 km). The simulated time-period is 2014 Dec – 2016 Dec (the first month used as spin-up). Tie et al. (2010) argued that the ratio of diameter of the analyzed city to model resolution should be at least 6:1, which means that in our case, 6 km or smaller horizontal grid step should be used to resolve the impact of urbanization for the cities chosen (see below). For Prague, which is modelled at 1 km, this is fulfilled. Other cities outside the inner 1 km nested domain are treated at coarser resolution but we can rely on the findings about the impact of emissions and model resolution on the species concentration: they found a rather small impact (Hodneborg et al., 2011; Markakis et al., 2015; Huszar et al., 2020a). For example, Wang et al. (2021a) showed that ozone production is reduced when high resolution is applied but the reduction is rather small, about 8% for ozone.

The ERA-interim reanalysis (Simmons et al., 2010) is used as forcing data. The 3 and 1 km domains are then driven by the corresponding parent domains with one-way nesting. Chemical boundary conditions are based on the CAM-chem global model data (Buchholz et al., 2019; Emmons et al., 2020). Landuse data was derived from the high resolution (100 m) CORINE CLC 2012 landcover data (<https://land.copernicus.eu/pan-european/corine-land-cover>) as well as from the United States Geological Survey (USGS) database for gridcells with no information from CORINE. In RegCM, fractional landuse is considered while in WRF, each gridcell is attributed the dominant landuse, which brings some accounting for the uncertainty related to the urban land-cover representation.

The European CAMS (Copernicus Atmosphere Monitoring Service) version CAMS-REG-APv1.1 inventory (Regional Atmospheric Pollutants; Granier et al., 2019) for year 2015 was used as anthropogenic emission data for areas outside Czech Republic. There, high resolution national data were adopted: the Register of Emissions and Air Pollution Sources (REZZO) dataset issued by the Czech Hydrometeorological Institute (www.chmi.cz) and the ATEM Traffic Emissions dataset provided by ATEM (Ateliér ekologických modelů – Studio of ecological models; www.atem.cz) were used. These data provide activity based (SNAP – Selected Nomenclature for sources of Air Pollution) annual emission totals of oxides of nitrogen (NO_x), volatile organic compounds (VOC), sulfur dioxide (SO₂), carbon monoxide (CO), PM_{2.5} and PM₁₀ (particles with diameter less than 2.5 and 10 μm). CAMS data are defined on a regular Cartesian lon–lat grid while the Czech datasets are provided as area, line (for road transportation) or point sources (in case of area sources these are usually irregular shapes corresponding to counties with resolution from a few 10 m to 1-2 km).

The Flexible Universal Processor for Modeling Emissions (FUME) emission model (<http://fume-ep.org/>; Benešová et al., 2018) is used to preprocess the mentioned emission inventories to CTM-ready emission files, including preprocessing the raw input files, the spatial remapping of the data into the model grid, chemical speciation, and time-disaggregation from annual



190 to hourly emissions. Category specific speciation factors and time-dissaggregation profiles were taken from (Passant, 2002) and (van der Gon et al., 2011), respectively. Emissions of biogenic origin are calculated offline using the MEGANv2.1 (Model of Emissions of Gases and Aerosols from Nature version 2.1) model (Guenther et al., 2012) based on RegCM and WRF meteorology. The necessary input for MEGAN including leaf-area index data, plant functional types and emission potentials were derived based on Sindelarova et al. (2014, 2022). It has to be mentioned here that along with the calculation of biogenic
195 VOC data, MEGAN also calculates the fluxes of soil-biogenic NO (nitrogen monoxide) emissions as a result of bacterial activity in soil according to (Yienger and Levy, 1995). As these emissions are a function of LAI and meteorological conditions, part of the “DBVOC” impact will be composed of soil-NO_x emissions modifications, although these modifications turned to be minor compared to the emission changes of biogenic VOC.

A key task was to isolate the emissions originating from urban areas (see further for details about the chosen cities). In this
200 regard, urban areas were identified based on the administrative boundaries of chosen cities. We used the GADM public database (<https://gadm.org>) for their definition. While masking of inventory emissions based on the GADM shapes corresponding to cities, it had to be ensured that the partition between the “city” and “non-city” portion of cross-boundary shapes is correctly calculated. For this purpose, the masking capability of FUME was adopted.

The cities chosen in the analysis are Berlin, Brussels, Budapest, Cluj-Napoca, Cologne, Frankfurt, Hamburg, Krakow, Lodz,
205 Lyon, Milan, Munich, Prague, Torino, Vienna, Warsaw, Wroclaw, Zagreb, Zurich. They are also highlighted in Fig. 1 including the 9 km domain terrain elevation. The choice of the cities regarded the same criteria as in Huszar et al. (2021): the size of the city comparable to one 9 km × 9 km gridcell, sufficient distance between cities to eliminate inter-city influences, minimal orographic variability to reduce orographic effects (Ganbat et al., 2015), no coastal cities to eliminate the effect of asymmetric landuse, like e.g. the sea-breeze effect (Ribeiro et al., 2018). Although strict emission control policies, these cities are still often
210 burdened with high air pollution for pollutants as NO₂ and O₃ (EEA, 2019; Khomeiko et al., 2021; Sokhi et al., 2022).

2.3 Model simulations

The study intends to evaluate the urbanization impact on air quality while we attempted to decompose the total impact into individual components listed in the Introduction. This requires to perform a series of model experiments with individual effects added one-by-one to reference state. In Huszar et al. (2018a, b) we performed similar decomposition for the urban induced
215 meteorological effects (i.e. the UCMF) and their impact on air-quality. Here we adopt this approach, but it will not concern the UCMF solely but the entire impact of urbanization while UCMF will be treated as one effect.

The simulations performed are summarized in the Tab. 1 and 2 for RCM and the underlying CTM simulations, respectively. A pair of simulation was performed with both RegCM and WRF with (“Urban”) and without (“Nourban”) considering urban land-surface. In the latter case, landuse was replaced by “crops” as the most common rural landuse type in the region analyzed.
220 While all RegCM simulations and CAMx simulations driven by RegCM were performed on nested domains (9 km, 3 km and 1 km), the WRF and CAMx simulations driven by WRF were done only over the parent 9 km domain as WRF served as a complementary model to account for the uncertainty in the driving meteorology, especially with regard to UCMF.



As for the CAMx simulations, they differ based on the inclusion of urbanized/rural land-surface, the UCMF (acting on both atmospheric chemistry in general and on BVOC fluxes) and the urban emissions. In this regard, we performed 6 experiments summarized in Tab. 2. The reference experiment called “ENNrrN” represents the hypothetical background state without urban emissions and with the urban land-surface replaced by rural land-surface in RCMs and CTM as well as in the BVOC model (MEGAN). In the next experiment “ENYrrN” only the urban emissions are considered (turned on). In the 3rd experiment “ENYurN” the urban landuse was “turned-on” for the dry-deposition in CAMx. The 4th experiment “ENYuuN” the urban landuse is “turned-on” also for the biogenic emission model. In the 5th experiment “ENYuuU”, both the urban landuse and the UCMF is accounted for the biogenic emissions model and finally, in the 6th experiment “EUYuuU”, all the urbanization-related effects are considered, representing the most realistic case.

In the first experiment where urban emissions are disregarded, we removed urban emissions only for the 19 cities chosen for the analysis (see Fig. 1). For the effect of rural-urban landuse transformation on meteorological conditions, dry-deposition and BVOC emissions, we replaced the urban land by rural one over the entire domain (i.e. not only for the cities chosen).

Mathematically, with respect to the rural-urban transformation (RUT), the concentration c_i of a pollutant i for a chosen city is given by:

$$c_i = c_{i,rural} + \Delta c_{i,RUT}, \quad (1)$$

where $c_{i,rural}$ is the average concentration before RUT and $\Delta c_{i,RUT}$ is the impact of urbanization.

In this study, we are concerned about the components of $\Delta c_{i,RUT}$.

$$\Delta c_{i,RUT} = \Delta c_{i,EMIS} + \Delta c_{i,MET} + \Delta c_{i,LU_D} + \Delta c_{i,BVOC}, \quad (2)$$

where $\Delta c_{i,EMIS}$, $\Delta c_{i,MET}$, $\Delta c_{i,LU_D}$ and $\Delta c_{i,BVOC}$ are the impacts of urban emissions, the impact of the urban canopy meteorological forcing, the impact of modified landuse on dry-deposition and the impact of modifications of BVOC emissions, denoted earlier as “DEMIS”, “DMET”, “DLU_D” and “DBVOC”. The $\Delta c_{i,BVOC}$ impact can further be decomposed into the part caused by modified land-cover (reduced vegetation in terms of changes in leaf-area-index LAI, “DBVOC_L”) and meteorological conditions (“DBVOC_M”):

$$\Delta c_{i,BVOC} = \Delta c_{i,BVOC_{LU}} + \Delta c_{i,BVOC_{MET}}. \quad (3)$$

These impacts will be calculated from the experiments listed in Tab. 2 in the following way (the experiment number is shown in the paranthesis):

$$\Delta c_{i,EMIS} = ENYrrN(2) - ENNrrN(1) \quad (4)$$

$$\Delta c_{i,MET} = EUYuuU(6) - ENYuuU(5) \quad (5)$$

$$\Delta c_{i,LU_D} = ENYurN(3) - ENYrrN(2) \quad (6)$$

$$\Delta c_{i,BVOC} = ENYuuU(5) - ENYurN(3) \quad (7)$$



3 Results

3.1 Validation

255 A brief account for validation is given here, as this model configuration (same input data, same domain) underwent a detailed
validation including both meteorology and air-quality in Huszar et al. (2020b) and Huszar et al. (2021). The only difference
here is that for the chemical simulations with CAMx, instead of version 6.50, version 7.10 was used which however does not
differ from the former version in principal components. The second difference is in the chemical mechanism, which is the
more advanced CB6 instead of the old CBV scheme used previously. For comparison with observations, the AirBase Euro-
260 pean air quality data (<http://www.eea.europa.eu/data-and-maps/data/aqereporting-1>) was used, while all urban and suburban
background stations were used from a subset of the analyzed cities.

In Fig. 2, the comparison of average monthly means of modelled and measured concentrations of the three analyzed pollutant
is shown. For NO₂, there is a generally acceptable match between the model and observation with model biases up to 10
µg m⁻³. While concentrations from Jan to Apr are usually underestimated, during summer, CAMx generates a positive bias,
265 except Berlin, where there is an underestimation of NO₂ from March to September and an overestimation during the rest of
the year. During late autumn the model bias is usually negative with large differences between cities.

For O₃, the model well captures the annual cycle with some overestimation of concentrations during late spring (by about
10-20 µg m⁻³) and an underestimation during late summer (by a similar magnitude). During winter, there is a small negative
(up to -10 µg m⁻³) model bias present.

270 Regarding SO₂, the model fails to capture well the annual cycle. During winter, model usually underestimates the concen-
trations up to 1-2 µg m⁻³ except Budapest and Berlin, when overestimation occurs in model. During summer, measured SO₂
concentrations are usually smaller and the model somewhat reflects this fact, but still large biases are present and the model is
unable to capture correctly the annual cycle for some cities (e.g. Budapest and Vienna).

3.2 The overall impact of individual components of RUT

275 Firstly, we evaluated the impact of individual components of the RUT as well as the total impact in terms of 2015-2016 DJF
and JJA averages (in case of ozone as summer average only), averaged across the chosen cities. Values are taken from gridbox
covering the center of a particular city. The results are shown in Fig. 3 as boxplots showing the 1st and 3rd quartiles as well as
the median values and the minimum and maximum. The analysis showed (as expected) that from the four contributors to RUT,
two are much stronger than the other two. Therefor in the plots, we separated them from the minors ones (including the total
280 impact).

For all three gas-phase pollutants, the impact of emissions (“DEMIS”) is the largest in magnitude in both seasons. For NO₂
it ranges (i.e. the 25% to 75% percentile) from 4 to about 8 ppbv and from 5 to 10 ppbv for JJA and DJF, respectively. For
SO₂, the numbers are somewhat smaller as cities, at least in the region in focus, are not so strong SO₂ emitters (compared to
NO₂): an increase by 0.4 to 1.5, and 0.8 to 1.6 ppbv for JJA and DJF, respectively, is seen. For O₃, the impact on the summer



285 maximum daily 8-hour average concentration (MDA8) is characterized by decrease due to titration (as expected) by 3 to 6
ppbv.

The impact of the urban canopy meteorological forcing (“DMET”) is characterized by a decrease for the primary pollutants:
for NO₂, the decrease is usually between 1 and 6 ppbv for JJA and between 1 and 3 ppbv in DJF with the maximum surpassing
zero meaning that in some cities, a slight increase was modelled. In case of SO₂, the impact of UCMF is smaller, up to 0.6
290 ppbv and 0.4 ppbv decrease in JJA and DJF, respectively. For O₃, the impact is an increase about 2 ppbv.

In case of minor contributors, the impact of BVOC is considerable for ozone only and as expected, for the other pollutants it
acts as a minor modulator of the overall chemistry (e.g. influencing the hydroxyl budget) therefor having a very small impact.
In case of NO₂, the impact is a slight increase by around 0.01 ppbv in JJA and negligible in winter. For SO₂, it is near zero in
both seasons. For ozone, which is directly influenced by biogenic emissions, the impact is a decrease by around 0.4 to 1 ppbv
295 as JJA average. The impact of modified dry-deposition due to urbanized landuse is characterized by an increase (0.02 to 0.08
ppbv) for NO₂ in JJA and an opposite impact in winter (around 0.01 to 0.04 ppbv decrease). For SO₂, the impact in summer
can be both negative and positive (from -0.01 to 0.01 ppbv) with the average near zero. In winter, there is a decrease by about
0.02 to 0.07. For ozone, the impact of landuse change is an increase between 1 and 2 ppbv.

Finally, the total impact is an increase for all pollutants and quantities: for NO₂ it is about 1-5 ppbv in JJA and 4-8 ppbv
300 in DJF, for SO₂ it ranges from 0 to 1 ppbv in JJA and about 0.5 to 1 ppbv in DJF. For JJA MDA8 ozone, the total impact is
characterized by an increase up to 2 ppbv.

3.3 The spatial distribution of the impacts

The boxplots presented above give an overview of the averaged impact across all the cities including the distribution around
the median value. To obtain a spatially resolved information of the individual impact, we plotted here also the 2-D distribution
305 of the individual contributors.

3.3.1 The impact of urban emissions (DEMIS)

In Fig. 4 the DJF and JJA average spatial impact of urban emissions (“DEMIS”) on the near-surface concentrations of NO₂,
SO₂ and O₃ is shown.

In case of NO₂, the impacts reaches 4-6 ppbv in the core of the cities and remains high over surrounding areas (up to 0.5
310 ppbv over large areas in DJF, especially in WRF driven simulations). In summer, the spatial extent of the emission impact is
smaller getting below 0.1 ppbv over rural areas. The result from Prague at high resolution reveals that the high emission impact
is concentrated to the very center of the city (reaching 4-6 ppbv).

For SO₂, there is a larger spread between cities with large contributions over Poland reaching 6 ppbv (in both seasons), while
for other cities, the contribution is smaller, up to 2-3 ppbv. The contribution over rural areas is large in Poland (up to 0.2 ppbv)
315 but remains below 0.1 ppbv in other regions. The impact of emissions over Prague reaches 1 ppbv in DJF with contributions
up to 0.1 ppbv in its vicinity. In summer, due to low emissions (SO₂ is emitted largely by heating) the contributions is very
small, reaching 0.5 ppbv in some hotspots within the city.



Ozone is usually titrated in city centres which corresponds to the impact of emission on its concentrations. They decreased over cities by up to 3-4 ppbv, while further from cities, where urban NO_x mix with rural emissions, ozone increase occur up to 1 ppbv as MDA8. Over Prague, the decrease is limited to the city area. Over its vicinity, the impact becomes positive with 0.5-1 ppbv increase (similar as seen for other cities).

3.3.2 The impact of modified meteorological conditions (DMET)

Fig. 5 presents the DJF and JJA average spatial impact of the urban canopy meteorological forcing (“DMET”) on the near-surface concentrations of NO₂, SO₂ and O₃.

In case of NO₂, while for RegCM/CAMx the impact is characterized usually by decrease by 1-2 ppbv with some urban areas showing even an increase (up to 2 ppbv), for WRF/CAMx a clear decrease occurs up to 3 ppbv. For Prague, the highest decreases are modelled in the city center reaching about 3 ppbv in summer and about 2 ppbv in DJF. In general, the winter impact is comparable to summer one (slightly stronger for WRF/CAMx).

For SO₂ the impact is weaker and constitutes both decreases (in cities) and increases (over their vicinity) with changes in the range -3 to 3 ppbv. In case of WRF/CAMx simulations, the impact is more straightforward with the decrease dominating reaching 3 ppbv in both seasons.

Finally, summer MDA8 ozone increases due to UCMF up to 2-3 over cities while over rural areas, a slight decrease is modelled up to 1 ppbv appearing in the RegCM/CAMx simulation. Over Prague, the largest increases are modelled in the city center reaching 2-3 ppbv.

3.3.3 The impact of dry-deposition modifications (DLUC_D)

The impact of the urban land-cover via modified dry-deposition (“DLU_D”) is plotted on Fig. 6. In general, the impacts are much smaller for NO₂ and SO₂ than seen for the emission or the UCMF impact for these pollutants above. For NO₂, the DJF and JJA impacts differ in sign (in accordance with the boxplots seen in Fig. 3) and the spatial distribution is somewhat different in WRF/CAMx than in RegCM/CAMx. In DJF, NO₂ concentrations decreased over cities by up to 0.04 ppbv, with some higher decreases over Italy (Milan) up to 0.1 ppbv. In the WRF driven experiment, some increases over the Benelux states are also seen reaching 0.06 ppbv. For Prague, the decrease is maximal in the city center reaching 0.04 ppbv. During JJA, the “DLU_D” impact is positive reaching 0.1 ppbv in both models with some slight decreases around Milan. Over Prague, the increase is even stronger and exceeds 0.05 ppbv.

For SO₂, there are clear decreases modelled during DJF reaching 0.1-0.2 ppbv over city centres. The impacts are slightly stronger in WRF driven CAMx runs and are about -0.03 ppbv over Prague’s center. During JJA, the SO₂ response is very small and positive in the RegCM/CAMx experiments up to 0.1 ppbv increase in some city centres, specially over eastern Europe where SO₂ emissions are higher. Decreases similar to the DJF impact remained in the WRF/CAMx simulation. Over Prague, the almost zero impact is modelled (lying between -0.01 and 0.01 ppbv with some positive impact around strong point sources north from the city).



350 A much stronger response to changes in dry-deposition is modelled for summer O_3 with a clear increase reaching 2 ppbv in city centres and being high over rural areas too (up to 1 ppbv increase). Over Prague, the increase is usually between 1.5-2 ppbv exceeding 2 ppbv in the very core of the city.

To facilitate the interpretation of the simulated responses of concentrations to “DLU_D”, we also mapped the geographical distribution of the “DLU_D” impact on the deposition velocities (DV is standardly provided on CAMx output), seen in Fig. 7
355 taken from the RegCM driven CAMx simulations (and not showing the Prague 1 km case). For NO_2 , dry deposition velocities decreased by around $0.2 \text{ mm}\cdot\text{s}^{-1}$ in DJF and a stronger decrease, reaching $-0.6 \text{ mm}\cdot\text{s}^{-1}$ in city centres is modelled in JJA. For SO_2 , the DJF and JJA maps differ in sign. For winter, deposition velocities increased in cities by up to $0.4\text{-}0.6 \text{ mm}\cdot\text{s}^{-1}$ while during summer, similar decreases are simulated compared to NO_2 (around -0.4 to $-0.6 \text{ mm}\cdot\text{s}^{-1}$). For O_3 , both seasons are characterized by decreases: by around $0.2 \text{ mm}\cdot\text{s}^{-1}$ in DJF and with a stronger decreases in city centres in JJA, reaching
360 $-1.5 \text{ mm}\cdot\text{s}^{-1}$. The WRF/CAMx impacts are very similar and are not shown here.

3.3.4 The impact of biogenic emissions (DBVOC)

The urbanization induced changes in BVOC emissions (via reduced vegetation cover and modified temperatures; “DBVOC”) and their consequent effect on summer ozone and NO_2 concentrations are plotted in Fig. 8. As BVOC emissions are of minor importance in winter and the effect on SO_2 are almost zero, we show only the summer impacts for these two pollutants.
365 For NO_2 , the “DBVOC” impact results in increases usually up to 0.06 ppbv while much stronger increases are modelled over northern Italy (around Milan) around 0.1 ppbv in both RegCM and WRF driven simulations. For Prague, the maximum increase is between 0.2-0.3 ppbv.

For O_3 , decreases are modelled reaching -1 ppbv over many cities and reaching -0.2 to -0.5 ppbv over rural areas (in the RegCM driven experiment). A stronger decrease is modelled (again) over northern Italy up to -2 ppbv over Milan. Prague is
370 characterized by a decrease usually between -0.5 and -1 ppbv.

The above presented impacts are the result of modified BVOC emissions, therefore we also plotted the summer changes of isoprene (ISOP) as a major component of such emissions due to “DBVOC”. As changes of these emissions is the result of two components constituted of vegetation change via LAI change (“DBVOC_L”) and modification of meteorological conditions (the UCMF; denoted “DBVOC_M” in the introduction), we plotted the two contributors separately in Fig. 9 as absolute and
375 relative change. We were also interested whether the reference with respect to which the change is calculated matters. In others words, what is the difference between the “DBVOC_L” calculated at rural (NOURBAN, see Tab. 1) meteorology and “DBVOC_L” calculated by urban meteorology (NOURBAN in Tab. 1). Similarly for “DBVOC_M”: it is calculated both with rural LAI and that adapted for urban conditions. The impact of vegetation change is an expected decrease in isoprene emissions by up to $15 \text{ mol}\cdot\text{km}^{-2}\cdot\text{hr}^{-1}$, with higher values over southern part of the domain, representing often a 80-90% decrease in
380 relative numbers, especially for larger and dense urban areas like Milan (Italy). For smaller urban areas the decrease is around -5 to -20% (many of the gridcells are only partly covered by urban areas and so the emission decrease is correspondingly small). As seen from the figure, the changes calculated at rural and urban meteorological conditions are very similar (the case with urban meteorology is slightly higher). Regarding the isoprene emission modifications due to UCMF, they are usually much



385 smaller (usually less than $0.05 \text{ mol.km}^{-2}\text{hr}^{-1}$ or less than 0.05% in relative numbers). At some urban areas over Germany and
over northern Italy and southern France, the change can reach 0.4 to $0.6 \text{ mol.km}^{-2}\text{hr}^{-1}$ peaking at $1\text{-}2 \text{ mol.km}^{-2}\text{hr}^{-1}$ over
Italian urban areas, representing a 5-10% relative increase. The “DBVOC_M” is somewhat smaller if calculated at urban land-
cover which is expected as the strongest meteorological modifications due to UCMF are over cities but in this case they affect
a non-vegetated surface which means smaller effects. In summary, the BVOC emission changes associated with vegetation
change are much more important than the modifications due to UCMF.

390 3.4 The diurnal variation of the impacts

Urban emissions have strong diurnal cycle caused by the typical cycle of human activities during the day. Moreover, the
urban land-surface triggered meteorological modifications (UCMF) have also a strong diurnal pattern, e.g. temperature is
impacted most during night, the wind impacts and turbulence modifications are the strongest during noon etc. (Huszar et al.,
2018a, 2020a). Thus it is clear that the individual components of RUT analyzed here are expected to have also a diurnal cycle.
395 Fig. 10 presents these cycles for the four components and three analyzed pollutants.

For NO_2 the diurnal pattern for the emissions impact (“DEMIS”) follows the expected shape with two peaks during morning
and evening rush hours reaching 10-12 ppbv and 9-11 ppbv in DJF and JJA, respectively. The diurnal cycle for the UCMF
impact (“DMET”) is negative throughout the whole day with peaking decrease during evening hours reaching -5 ppbv and -8
ppbv in DJF and JJA, respectively. In case of the impact of modified dry-deposition (“DLU_D”) it has a somewhat different
400 pattern in two seasons. In DJF, it is negative throughout the day with a strong peak during morning hours (-0.04 ppbv) and
a smaller evening peak (-0.03 ppbv). In summer, this impact is positive almost during the whole day with two peaks during
morning and early evening hours reaching 0.18-0.2 ppbv, while during night, the impact can be slightly negative up to -0.04
ppbv. The impact of BVOC changes (“DBVOC”) is very small during winter with negative values peaking at less than -0.01
ppbv. During summer, the impact is stronger with a clear positive peak during evening hours reaching 0.06 ppbv.

405 In case of SO_2 , the diurnal pattern for the impact of emissions and UCMF is similar to NO_2 . The emissions impact is peaking
at morning and evening rush hours for JJA reaching 2.6-2.8 ppbv while in DJF, the maximum impact is reached at evening
hours and the impact remains high during the whole night (around 2.5-3 ppbv). The “DMET” impact is negative with an
evening peak reaching -0.06 and -0.03 in DJF and JJA, respectively. The impact on dry-deposition is negative in JJA with a
maximum impacts during morning and evening hours reaching -0.05 to -0.07 ppbv. During JJA, the impact is positive during
410 day with increases up to 0.03 ppbv and decreases during night up to -0.04 ppbv. We already saw in the boxplots and also
expected that the impact of BVOC emission change has an almost zero effect on SO_2 , which is directly not tight chemically
with VOC chemistry.

Finally, for ozone, the impact of urban emissions is a decrease with two peaks during morning and evening hours reaching
-10 to -12 ppbv in DJF and -8 to -10 ppbv in JJA. The impact of UCMF shows a clear increase peaking during evening hours
415 reaching around 5 and 10 ppbv during DJF and JJA, respectively. The impact of modifications of dry-deposition is positive
throughout the day with a strong peak during noon to early evening hours - during DJF, the peaks reaches 0.2 ppbv while a



much stronger increase is modelled during summer reaching 1.5-2 ppbv increase. The impact of BVOC changes on ozone are virtually zero during DJF and are negative during JJA with a peak decrease around noon reaching -1 ppbv.

We evaluated also the diurnal cycle of impact on deposition velocities, as this helps the interpretation of the “DLU_D”. In Fig. 11 the 2015-2016 winter and summer average of this cycle for the three analyzed pollutants is plotted. In case of NO₂, DV are reduced when turning rural landuse into urban one and the maximum decrease occurs during noon to early afternoon reaching -0.4 mm.s⁻¹ in DJF and a stronger decrease reaching -3 mm.s⁻¹ in JJA while during night, the change is close to zero. Very similar decreases are calculated for ozone with somewhat smaller nocturnal decrease in DJF and a weaker decrease during summer peak values. For SO₂, the impact on DV is different between DJF and JJA. During DJF, DV increases by 0.6 mm.s⁻¹ during night, while a smaller increase is calculated around noon time (0.2 mm.s⁻¹). During JJA, DV change for SO₂ is slightly above zero and a strong negative peak occurs during the day reaching about -1.5 to -2 mm.s⁻¹.

4 Discussion and conclusions

We presented a novel, component based analysis of the different contributors to the overall impact of urbanization (what we called here the rural-urban-transformation; RUT) on gas-phase air pollutant concentrations. We identified four contributors to RUT, namely the impact of urban emissions (“DEMIS”), the impact of the urban canopy meteorological forcing (“DMET”) on pollutant chemistry and transport, the impact of modified dry-deposition due to the land-cover modifications (“DLU_D”) and the impact of modified biogenic emissions due to modified land-cover (and associated vegetation change) and modified meteorological conditions (“DBVOC”). By performing multiple simulations where each contributor of RUT was added one-by-one to the reference state representing a land without urban land-cover and urban emissions, we could quantify them individually.

The validation showed a reasonable range of model biases and the annual cycles of pollutant concentrations were well captured. Overall the biases are smaller than in Huszar et al. (2021) for NO₂, i.e. the underestimation seen there is greatly reduced and smaller than seen in other similar studies (Karlický et al., 2017; Tucek et al., 2012). Huszar et al. (2021) attributed the NO₂ underestimation to low urban emission estimates, however in our study here we used the same emission inventory data, only the chemistry mechanism was updated (from CB-V to CB6r5). This suggest a great importance of this decision and a better representation of tropospheric NO_x chemistry. Indeed, CB6 was added to CAMx to take into account the long-lived organic compounds formed by peroxy radical reactions which serve as an inhibitor of OH recycling and reduces NO_x removal by OH oxidation (Cao et al., 2021). Previously, Luecken et al. (2019) also found a better model performance for reactive nitrogen when CB6 was used instead of CB-V. The slight deviation of the monthly cycle of observed values is probably caused by not correct annual temporal disaggregation profiles. Monthly ozone values are well represented by our model system giving smaller biases than in Huszar et al. (2016a, 2020b), which was due to strong nighttime bias and overall weak performance in night-time chemical conditions (see also Zanis et al., 2011; Huszar et al., 2020b, ;). The improvement can be most probably attributed, again, to improvements in NO_x-VOC-Ozone chemistry in CB6 with respect to CB-V; a similar conclusion was made by Cao et al. (2021) too. Further, our results show a similar model-observation agreement than the large online-coupled



450 model comparison study by Im et al. (2015). In case of SO_2 , the model is rather unable to correctly resolve the annual cycle of
near-surface concentrations. We saw this behavior in a similar manner in Huszar et al. (2016a) or in Karlický et al. (2017) too
and points to deficiencies in the annual profile used to time-disaggregate annual emissions to monthly-ones. The SO_2 biases
can be caused also by wrong vertical turbulent mixing as large quantities of this pollutants are emitted from tall stacks (as point
sources) and they have to mixed down to the layer above the surface, which is greatly influenced by the model representation
455 of vertical eddy-diffusivities. These are especially important in urban areas (Huszar et al., 2020a). In summary, we did not
identify substantial model biases in simulating near-surface concentrations of the analyzed pollutants which hints that the
effect of urban emissions is well captured too (e.g. Huszar et al. (2021) strongly underestimated NO_2 which suggest that the
impact of urban emissions, at least for this pollutant, are underestimated too in their study).

The total impact of urbanization on NO_2 was calculated to around $3(1\div 5)$ ppbv in summer and $6(3\div 8)$ ppbv in winter.
460 These numbers are smaller than the annual mean contributions calculated for 2001-2010 in Huszar et al. (2016a), higher
contributions were also modelled by Im and Kanakidou (2012) however both simulated only the effect of urban emissions
without considering the effect of the UCMF which decreases near-surface concentrations (see further). The total impact on SO_2
is between 0 and 1 ppbv in summer and 0.5-1.3 in winter, which is a smaller contribution than in Huszar et al. (2016a) due to
much lower sulfur emissions in 2015 compared to the 2005 emissions used there and due to not considering the UCMF effects.
465 The total average contribution for ozone summer MDA8 is about $1.5(0\div 2)$ ppbv. In Huszar et al. (2016a) for an ensemble of
central European cities and Im et al. (2011a, b) for Mediterranean cities decrease of ozone was shown (and increase over rural
areas, similar to our results), but they accounted for only the urban emission impact. Indeed, the urbanization via the UCMF
increases ozone concentrations (Kim et al., 2015; Huszar et al., 2018a, 2020b) which can offset the decrease seen solely due
to urban emissions. Indeed, for all three pollutants, the effect of emissions (“DEMIS”) is stronger than the total effect of
470 urbanization (“DTOT”) due to the strong modulating effect of the urban canopy meteorological forcing. As already calculated
by many (e.g. Wang et al., 2007, 2009; Struzewska and Kaminski, 2012; Zhu et al., 2015; Huszar et al., 2020a), the vertical
eddy-diffusion is the most important component of UCMF which is strongly enhanced above urban areas. Consequently, it
leads to reduced near-surface concentrations of primary pollutants (e.g. NO_2 , SO_2) and an increase of ozone due to reducing
the titration by NO (Escudero et al., 2014; Xie et al., 2016a, b).

475 As for the impact of UCMF (“DMET”) alone, our simulations showed a decrease by about 2 ppbv for NO_2 , by 0.2-0.3 for
 SO_2 (for both seasons) and an increase of summer MDA8 ozone by about 2 ppbv. These numbers well fit previous findings
in Sarrat et al. (2006); Struzewska and Kaminski (2012); Kim et al. (2015); Huszar et al. (2018a, 2020b). They concluded
that three main components play the most important role in UCMF: increased urban temperatures, decreased windspeeds and
increased vertical turbulent diffusion. While elevated surface temperatures favor photochemistry, they also result in stronger
480 dry-depositon as showed by Huszar et al. (2018a). Regarding the wind-speed and turbulence effect, they are counteracting
which is seen in our results too especially for SO_2 . For some of the cities, the impact is positive meaning that the reduction
of wind results in the emitted material remaining close to the sources. This was previously seen also by Huszar et al. (2018b)
where the turbulence and wind effects were strongly competing for this pollutant. Our results also showed that the trade-off
between wind and turbulence effects depends also on how the model simulates the UCMF components and in our results, WRF



485 produced somewhat stronger increase in turbulence due to UCMF and weak wind reduction compared to RegCM. For ozone,
the UCMF increased ozone by 2 ppbv, which is in line with previous finding in Huszar et al. (2018a), although they included
also the effect of BVOC emissions modifications which was treated here separately (see further). Due to urbanization, similar
increase was obtained by Martilli et al. (2003); Jiang et al. (2008); Xie et al. (2016a) or Jacobson et al. (2015). Some authors
found somewhat larger increases for ozone (e.g. Ryu et al., 2013, for Seoul), but they adopted higher resolutions for the cities
490 in focus and thus obtained higher peak impacts in urban centres (as seen in e.g. Huszar et al., 2020b, too).

The diurnal pattern for the “DMET” impact shows a very characteristic pattern. In case of primary pollutants (NO_2 and
 SO_2) the decrease is strongest during evening hours. This can be explained by the largest absolute values during evening hours
which is further closely related to the maximum impact of emissions – a similar finding was found by Huszar et al. (2018a)
and also by Huszar et al. (2018b) for primary aerosol components. Indeed, the amount of gases transported due to enhanced
495 turbulence is proportional to the absolute concentrations and these are highest during evening hours due to strong emissions
during transport rush hours. For ozone, the diurnal pattern contains a maximum during evening hours corresponding to largest
impact on NO_2 . This justifies the argument that the UCMF induced ozone increase is mainly caused by reduced NO_x due to
strong urban dilution and consequent reduced titration.

Besides the strong and well documented air-quality effects of urban emissions (“DEMIS”) and UCMF (“DMET”), our study
500 also looked at two other components of RUT, which were expected to be smaller but which were not yet quantified in detail.
Our study, at least by the knowledge of the authors, is among the firsts that explicitly investigated the effect of urbanization
from the perspective of change in dry-deposition (“DLU_D”) and we also looked at the effect of the urbanization induced
changes in BVOC emissions, which was examined only partly in previous studies (e.g. Huszar et al., 2018a; Li et al., 2019).

The impact due to modified dry-deposition shows for NO_2 a distinct picture between summer and winter. For both seasons,
505 reduced deposition velocities were modelled with stronger decreases in summer (the WRF driven CAMx results are not shown
as they differ from the RegCM driven only slightly). Reduced deposition velocities result in higher concentrations which is
opposite to what was modelled. To better understand what controls the NO_2 budget we have to consider the simultaneous
effect of ozone changes due to changes in dry-deposition. Our results showed strong increases in ozone concentrations caused
by suppressed dry-deposition (for winter too, not shown in this manuscript). This is expected as many studies showed strong
510 dependence of both ozone concentrations on ozone deposition (Tao et al., 2013; Park et al., 2014) and the ozone deposition on
the landuse information (McDonald-Buller et al., 2001). When examining the concentration response to changed dry-deposition,
one has to consider the indirect impact due to other influenced pollutants and probably pollutants responsible for NO_2 removal
(e.g. by reaction $\text{NO}_2 + \text{OH}$ forming nitric acid or by $\text{NO}_2 + \text{O}_3$ forming nitrate radical) were impacted by weaker dry-
deposition (as seen for ozone) resulting in decreases in NO_2 , outweighing the direct impact of dry-deposition, as seen for
515 winter. Another factor playing role in decreases of NO_2 can be in the much larger (by 50%) deposition velocities for nitric
acid (HNO_3) in the Zhang model for urban landuse type compared to crops or similar rural landuse (i.e. “nourban” case).
Large dry-deposition for HNO_3 in turn results in decrease of this compound which reduces the recycling of NO_2 from it (by
photolysis). On the other hand in summer, such effects can amplify the impact. In this season the deposition induced ozone



changes played probably a role in the NO_2 budget. It has to realized that a major pathway of NO_2 in cities is oxidation of NO
520 with ozone ($\text{NO} + \text{O}_3 \rightarrow \text{NO}_2$). Increased ozone concentrations thus results in more NO oxidizing to NO_2 .

In case of sulfur dioxide, deposition increased in winter which resulted in clear decrease of near-surface concentration. The
dry-deposition of sulfur strongly differs between wet a dry-soils (Hardacre et al., 2021) and according to Zhang et al. (2003)
which provided the dry-deposition scheme we adopted the deposition velocities (DV) are higher for urban areas than for crops
or similar rural landuse type (which was considered in the “nourban” case). In winter, soils are very often wet which could
525 result in increase in DVs (especially during night as seen our results) and the consequent decrease of concentrations. During
summer, DVs decreased for SO_2 , however, there is no clear increase of concentrations, i.e. almost no change in RegCM driven
simulations and even some decrease in the WRF driven ones. This can be explained again by the impact of deposition on other
chemical species which cause removal of SO_2 , typically the oxidation by OH radical.

The impact of BVOC emission changes (“DBVOC”) straightforward and expected for ozone, i.e. a decrease by 0.5-1 ppbv.
530 BVOC emissions decreased due to urbanization related reduction of vegetation (i.e. reduction of vegetation fraction and leaf-
area-index) and increased due to higher urban temperatures (within the action of the UCMF). This latter effect was smaller
resulting in the dominance of the first effect and an overall decrease of emissions, a similar results as in e.g. Li et al. (2019).
As ozone chemistry in cities in Europe (and also North American and Asian megacities) is characterized by VOC-controlled
regime with high NO_x/VOC ratio (Beekmann and Vautard, 2010; Xue et al., 2014), ozone quickly responds to changes in
535 VOC emissions, i.e. it decreases with decreasing BVOC emissions. This is in accordance with previous studies: e.g. Song et
al. (2008) reported an 10% decrease in ozone concentrations. The reduction in ozone was shown to be largest during daytime,
which is in accordance with the largest BVOC emissions. Previously, Huszar et al. (2018a) reported ozone increases due to
BVOC changes due to UCMF alone (i.e. not considering the impact of reduced vegetation) of order of up to 0.1 ppbv. Our
study showed that if vegetation modifications related to urbanization are added, this increase is out-weighted by a much stronger
540 decrease due to lower BVOC emissions.

Simultaneously with the “DBVOC” related ozone decrease, we calculated a small summer increase of NO_2 by about 0.01
ppbv. This cannot be explained by a potentially reduced NO concentrations and suppressed NO_2 formation with the reaction of
ozone (titration) as NO also increased slightly as the result of “DBVOC” (not shown explicitly in this study) and moreover,
soil NO_x emissions in MEGAN also decreased slightly due to urban landuse transformation. Reduced BVOC emissions results
545 in reduced peroxy-radical (RO_2) concentrations, which is an important oxidation pathway to form NO_2 from NO (Geng et al.,
2011) and would result in decrease of NO_2 . There must therefore exist another compensating mechanism responsible for NO_x
increase and this is probably the reduced concentrations of NO_x sinks. One of the important urban contributors to this are the
PANs (peroxy-acetyl nitrates) and as biogenic VOCs are a major contributor to urban PAN concentrations, it can be expected
that with decreased BVOC emissions, the PAN sink is reduced resulting in higher NO_x concentrations (Fischer et al., 2014;
550 Toma et al., 2019). Another reasons can lie in the reaction with OH radical, which is reduced if ozone is reduced. In short,
the relatively small positive NO_2 response to urbanization induced biogenic emissions changes is a probably a simultaneous
acting of multiple indirect chemical pathways and deeper process based analysis should be performed to explicitly show the
contribution and trade-off of each of them.



To summarize our finding, we showed on an ensemble 19 European cities that the most important contributors to the impact
555 of rural-to-urban transformation are the urban emissions themselves (increase concentrations for nitrogen dioxide and sulfur
dioxide and decrease for ozone) and the urban canopy meteorological forcing (decreases the concentration of primary pol-
lutants and increases those of ozone). These are two major drivers of urban air pollution and they have to be accounted for
simultaneously as the impact of urban emissions without considering UCMF can lead to overestimation of the impact (Huszar
et al., 2021). Additionally, we quantified two weaker contributors. The effect of modified landuse on dry-deposition and the ef-
560 fect of modified biogenic emissions have two orders of magnitude weaker magnitude than emissions and the UCMF. However,
we showed that for summer ozone, these are strong and of comparable order than the two major impacts. In other words, when
analyzing the overall impact of urbanization on air-pollution for ozone, all four components has to be accounted for while for
primary pollutants (i.e. NO₂ and SO₂), the two minor contributors can be neglected.

Finally, it has to be noted that some secondary effects of modified pollutant concentrations can potentially play also a role
565 via the direct and indirect radiative effect of emissions. The direct effect of aerosols can alter photolysis rates and temperatures
influencing air chemistry (Han et al., 2020; Wang et al., 2022). It was further shown by many that aerosol emitted by urban
areas modulates the vertical structure of the atmosphere and convection resulting in modification of stability and/or convection
(Miao et al., 2020; Slater et al., 2022; Fan et al., 2020; Yu et al., 2020) which in turn can modify the vertical mixing or the
precipitation (Zhou et al., 2020; López-Romero et al., 2021), which finally feedbacks to influence on species concentration
570 via wet-deposition and mixing. Our study was an offline coupled one meaning that no feedbacks from species concentrations
via radiation and cloud/rain microphysics were accounted for. These studies however indicate, that to obtain an even more
comprehensive picture of the total RUT impact, these secondary effects has to be taken into account too in the future.

Code and data availability. The RegCM4.7 model is freely available for public use at <https://gforge.ictp.it/gf/download/frsrelease/259/1845/RegCM-4.7.0.tar.gz> (Giuliani, 2021). CAMx version 7.10 is available at <http://www.camx.com/download/default.aspx> (ENVIRON, 2020). The RegCM2CAMx
575 meteorological preprocessor used to convert RegCM outputs to CAMx inputs and the MEGAN v2.10 code as used by the authors is available
upon request from the main author. The complete model configuration and all the simulated data (3-dimensional hourly data) used for the
analysis are stored at the Dept. of Atmospheric Physics of the Charles University data storage facilities (about 3TB) and are available upon
request from the main author.

Author contributions. PH created the concept and designed the experiments, PH and JK performed the model simulations, LB and ML
580 contributed to input data preparation, model configuration and analysis of the outputs, APPP contributed to the validation, ALL authors
contributed to the manuscript

Competing interests. The authors declare that they have no conflict of interest.



Acknowledgements. This work has been funded by the Czech Science Foundation (GACR) project No. 19-10747Y and partly by projects PROGRES Q47 and SVV 260581/2020 – Programmes of Charles University. We further acknowledge the CAMS-REG-APv1.1 emissions dataset provided by the Copernicus Atmosphere Monitoring Service, the Air Pollution Sources Register (REZZO) dataset provided by the Czech Hydrometeorological Institute and the ATEM Traffic Emissions dataset provided by ATEM (Studio of ecological models). We also acknowledge the providers of AirBase European Air Quality data (<http://www.eea.europa.eu/data-and-maps/data/aqereporting-1>).

585



References

- Beekmann, M. and Vautard, R.: A modelling study of photochemical regimes over Europe: robustness and variability, *Atmos. Chem. Phys.*, 10, 10067–10084, doi:10.5194/acp-10-10067-2010, 2010.
- 590 Benešová, N., Belda, M., Eben, K., Geletič, J., Huszár, P., Juruš, P., Krč, P., Resler, J. and Vlček, O.: New open source emission processor for air quality models, In Sokhi, R., Tiwari, P. R., Gállego, M. J., Craviotto Arnau, J. M., Castells Guiu, C. and Singh, V. (eds) Proceedings of Abstracts 11th International Conference on Air Quality Science and Application, doi: 10.18745/PB.19829. (pp. 27). Published by University of Hertfordshire. Paper presented at Air Quality 2018 conference, Barcelona, 12-16 March, 2018.
- 595 Bougeault, P. and Lacarrère, P.: Parameterization of orography-induced turbulence in a meso-beta-scale model, *Mon. Weather Rev.*, 117, 1872-1890, 1989.
- Burkholder, J.B., S.P. Sander, J.P.D. Abbatt, J.R. Barker, R.E. Huie, C.E. Kolb, M.J. Kurylo, V.L. Orkin, D.M. Wilmouth and P.H. Wine. 2015. Chemical kinetics and photochemical data for use in atmospheric studies: evaluation number 18. JPL Publication 15-10, Jet Propulsion Laboratory, Pasadena, CA, available at <http://jpldataeval.jpl.nasa.gov>, 2019.
- 600 Butler, T. M. and Lawrence, M. G.: The influence of megacities on global atmospheric chemistry: a modelling study, *Environ. Chem.*, 6, 219–225, doi:10.1071/EN08110, 2009.
- Buchholz, R. R., Emmons, L. K., Tilmes, S. and The CESM2 Development Team: CESM2.1/CAM-chem Instantaneous Output for Boundary Conditions. UCAR/NCAR - Atmospheric Chemistry Observations and Modeling Laboratory. Subset used Lat: 10 to 80, Lon: -20 to 50, December 2014 - January 2017, Accessed: 19/09/2019, <https://doi.org/10.5065/NMP7-EP60>, 2019.
- 605 Byun, D. W. and Ching, J. K. S.: Science Algorithms of the EPA Model-3 Community Multiscale Air Quality (CMAQ) Modeling System. Office of Research and Development, U.S. EPA, North Carolina, 1999.
- Cao, L., Li, S., and Sun, L.: Study of different Carbon Bond 6 (CB6) mechanisms by using a concentration sensitivity analysis, *Atmos. Chem. Phys.*, 21, 12687–12714, <https://doi.org/10.5194/acp-21-12687-2021>, 2021.
- Chen, S. and Sun, W.: A one-dimensional time dependent cloud model, *J. Meteorol. Soc. Jpn.*, 80, 99-118, 2002.
- 610 Cherin, N., Roustan, Y., Musson-Genon, L., and Seigneur, C.: Modelling atmospheric dry deposition in urban areas using an urban canopy approach, *Geosci. Model Dev.*, 8, 893–910, <https://doi.org/10.5194/gmd-8-893-2015>, 2015.
- Đoubalová, J.; Huszár, P.; Eben, K.; Benešová, N.; Belda, M.; Vlček, O.; Karlický, J.; Geletič, J.; Halenka, T.: High Resolution Air Quality Forecasting Over Prague within the URBI PRAGENSI Project: Model Performance During the Winter Period and the Effect of Urban Parameterization on PM, *Atmosphere*, 11, 625, 2020.
- 615 European Environment Agency: Air quality in Europe — 2019 report, EEA Report No 10/2019, doi:10.2800/822355, 2019.
- Emmons, L. K., Schwantes, R. H., Orlando, J. J., Tyndall, G., Kinnison, D., Lamarque, J.F., et al.: The Chemistry Mechanism in the Community Earth System Model version 2 (CESM2), *J. Adv. Model. Earth Sys.*, 12, e2019MS001882. <https://doi.org/10.1029/2019MS001882>, 2020.
- ENVIRON, CAMx User's Guide, Comprehensive Air Quality model with Extensions, version 7.10, www.camx.com, Novato, California, 620 2020.
- Escudero, M., Lozano, A., Hierro, J., del Valle, J., and Mantilla, E.: Urban influence on increasing ozone concentrations in a characteristic Mediterranean agglomeration, *Atmos. Environ.*, 99, 322–332, doi:10.1016/j.atmosenv.2014.09.061, 2014.
- Fan, J., Zhang, Y., Li, Z., Hu, J., and Rosenfeld, D.: Urbanization-induced land and aerosol impacts on sea-breeze circulation and convective precipitation, *Atmos. Chem. Phys.*, 20, 14163–14182, <https://doi.org/10.5194/acp-20-14163-2020>, 2020.



- 625 Finardi, S., Silibello, C., D'Allura, A., and Radice, P.: Analysis of pollutants exchange between the Po Valley and the surrounding European region, *Urban Climate*, 10, 682–702, doi:10.1016/j.uclim.2014.02.002, 2014.
- Fischer, E. V., Jacob, D. J., Yantosca, R. M., Sulprizio, M. P., Millet, D. B., Mao, J., Paulot, F., Singh, H. B., Roiger, A., Ries, L., Talbot, R. W., Dzepina, K., and Pandey Deolal, S.: Atmospheric peroxyacetyl nitrate (PAN): a global budget and source attribution, *Atmos. Chem. Phys.*, 14, 2679–2698, https://doi.org/10.5194/acp-14-2679-2014, 2014.
- 630 Folberth, G. A., Butler, T. M., Collins, W. J., and Rumbold, S. T.: Megacities and climate change – A brief overview, *Environ. Pollut.*, 203, 235–242, http://dx.doi.org/10.1016/j.envpol.2014.09.004, 2015.
- Galmarini, S., Makar, P., Clifton, O. E., Hogrefe, C., Bash, J. O., Bellasio, R., Bianconi, R., Bieser, J., Butler, T., Ducker, J., Flemming, J., Hodzic, A., Holmes, C. D., Kioutsioukis, I., Kranenburg, R., Lupascu, A., Perez-Camanyo, J. L., Pleim, J., Ryu, Y.-H., San Jose, R., Schwede, D., Silva, S., and Wolke, R.: Technical note: AQMEII4 Activity 1: evaluation of wet and dry deposition schemes as an integral part of regional-scale air quality models, *Atmos. Chem. Phys.*, 21, 15663–15697, https://doi.org/10.5194/acp-21-15663-2021, 2021.
- 635 Ganbat, G., Baik, J. J. and Ryu, Y. H.: A numerical study of the interactions of urban breeze circulation with mountain slope winds, *Theor. App. Clim.*, 120(1-2), 123–135, 2015.
- Gao, J. and O'Neill B. C.: Mapping global urban land for the 21st century with data-driven simulations and Shared Socioeconomic Pathways, *Nature Com.*, 11, 2302, https://doi.org/10.1038/s41467-020-15788-7, 2020.
- 640 Geng, F., Tie, X., Guenther, A., Li, G., Cao, J., and Harley, P.: Effect of isoprene emissions from major forests on ozone formation in the city of Shanghai, China, *Atmos. Chem. Phys.*, 11, 10449–10459, https://doi.org/10.5194/acp-11-10449-2011, 2011.
- Giorgi, F., Coppola, E., Solmon, F., Mariotti, L., Sylla, M., Bi, X., Elguindi, N., Diro, G. T., Nair, V., Giuliani, G., Cozzini, S., Guettler, I., O'Brien, T. A., Tawfi, A. B., Shalaby, A., Zakey, A., Steiner, A., Stordal, F., Sloan, L., and Brankovic, C.: RegCM4: model description and preliminary tests over multiple CORDEX domains, *Clim. Res.*, 52, 7–29, 2012.
- 645 ICTP: The Regional Climate Model version 4.7 source code (provided by Graziano Giuliani), https://github.com/ictp-esp/RegCM/releases?after=4.7.9 (last access 2021/03/31), 2021.
- van der Gon, H. D., Hendriks, C., Kuenen, J., Segers, A. and Visschedijk, A.: Description of current temporal emission patterns and sensitivity of predicted AQ for temporal emission patterns. EU FP7 MACC deliverable report D_D-EMIS_1.3, http://www.gmes-atmosphere.eu/documents/deliverables/d-emis/MACC_TNO_del_1_3_v2.pdf, 2011.
- 650 Granier, C.S., Darras, H., Denier van der Gon, J., Doubalova, N., Elguindi, B., Galle, M., Gauss, M., Guevara, J.-P., Jalkanen, J. and Kuenen, C.: The Copernicus Atmosphere Monitoring Service Global and Regional Emissions; Report April 2019 version [Research Report]; ECMWF: Reading, UK, doi:10.24380/d0bn-kx16, 2019.
- Grell, G.: Prognostic evaluation of assumptions used by cumulus parameterizations, *Mon. Weather Rev.*, 121, 764–787, 1993.
- Guenther, A., Karl, T., Harley, P., Wiedinmyer, C., Palmer, P. I., and Geron, C.: Estimates of global terrestrial isoprene emissions using MEGAN (Model of Emissions of Gases and Aerosols from Nature), *Atmos. Chem. Phys.*, 6, 3181–3210, https://doi.org/10.5194/acp-6-3181-2006, 2006.
- 655 Guenther, A. B., Jiang, X., Heald, C. L., Sakulyanontvittaya, T., Duhl, T., Emmons, L. K., and Wang, X.: The Model of Emissions of Gases and Aerosols from Nature version 2.1 (MEGAN2.1): an extended and updated framework for modeling biogenic emissions, *Geosci. Model Dev.*, 5, 1471–1492, https://doi.org/10.5194/gmd-5-1471-2012, 2012.
- 660 Guttikunda, K. S., Carmichael, G. R., Calori, G., Eck, C., and Woo, J.-H.: The contribution of megacities to regional sulfur pollution in Asia, *Atmos. Environ.*, 37, 11–22, doi:10.1016/S1352-2310(02)00821-X, 2003.



- Guttikunda, S. K., Tang, Y., Carmichael, G. R., Kurata, G., Pan, L., Streets, D. G., Woo, J.-H., Thongboonchoo, N., and Fried, A.: Impacts of Asian megacity emissions on regional air quality during spring 2001, *J. Geophys. Res.*, 110, D20301, doi:10.1029/2004JD004921, 2005.
- 665 Han, W., Li, Z., Wu, F., Zhang, Y., Guo, J., Su, T., Cribb, M., Fan, J., Chen, T., Wei, J., and Lee, S.-S.: The mechanisms and seasonal differences of the impact of aerosols on daytime surface urban heat island effect, *Atmos. Chem. Phys.*, 20, 6479–6493, <https://doi.org/10.5194/acp-20-6479-2020>, 2020.
- Hardacre, C., Mulcahy, J. P., Pope, R. J., Jones, C. G., Rumbold, S. T., Li, C., Johnson, C., and Turnock, S. T.: Evaluation of SO₂, SO₄²⁻ and an updated SO₂ dry deposition parameterization in the United Kingdom Earth System Model, *Atmos. Chem. Phys.*, 21, 18465–18497, <https://doi.org/10.5194/acp-21-18465-2021>, 2021.
- 670 Hodnebrog, Ø., Stordal, F., and Berntsen, T. K.: Does the resolution of megacity emissions impact large scale ozone?, *Atmos. Environ.*, 45, 6852–6862, 2011.
- Holtslag, A. A. M., de Bruijn, E. I. F., and Pan, H.-L.: A high resolution air mass transformation model for shortrange weather forecasting, *Mon. Wea. Rev.*, 118, 1561–1575, 1990.
- Hong, S.-Y., Dudhia, J. and Chen, S.-H.: A Revised Approach to Ice Microphysical Processes for the Bulk Parameterization of Clouds and Precipitation, *Month. Weather Rev.*, 132, 103–120., [http://dx.doi.org/10.1175/1520-0493\(2004\)132<0103:ARATIM>2.0.CO;2](http://dx.doi.org/10.1175/1520-0493(2004)132<0103:ARATIM>2.0.CO;2), 2004.
- 675 Hood, C., MacKenzie, I., Stocker, J., Johnson, K., Carruthers, D., Vieno, M., and Doherty, R.: Air quality simulations for London using a coupled regional-to-local modelling system, *Atmos. Chem. Phys.*, 18, 11221–11245, <https://doi.org/10.5194/acp-18-11221-2018>, 2018.
- Huszár, P., Cariolle, D., Paoli, R., Halenka, T., Belda, M., Schlager, H., Miksovsky, J., and Pisoft, P.: Modeling the regional impact of ship emissions on NO_x and ozone levels over the Eastern Atlantic and Western Europe using ship plume parameterization, *Atmos. Chem. Phys.*, 10, 6645–6660, doi:10.5194/acp-10-6645-2010, 2010.
- 680 Huszar, P., Miksovsky, J., Pisoft, P., Belda, M., and Halenka, T.: Interactive coupling of a regional climate model and a chemistry transport model: evaluation and preliminary results on ozone and aerosol feedback, *Clim. Res.*, 51, 59–88, doi:10.3354/cr01054, 2012.
- Huszár, P., Teyssèdre, H., Michou, M., Voldoire, A., Olivie, D. J. L., Saint-Martin, D., Cariolle, D., Senesi, S., Salas Y Melia, D., Alias, A., Karcher, F., Ricaud, P., and Halenka, T.: Modeling the present and future impact of aviation on climate: an AOGCM approach with online coupled chemistry, *Atmos. Chem. Phys.*, 13, 10027–10048, doi:10.5194/acp-13-10027-2013, 2013.
- 685 Huszar, P., Halenka, T., Belda, M., Zak, M., Sindelarova, K., and Miksovsky, J.: Regional climate model assessment of the urban land-surface forcing over central Europe, *Atmos. Chem. Phys.*, 14, 12393–12413, doi:10.5194/acp-14-12393-2014, 2014.
- Huszar, P., Belda, M., and Halenka, T.: On the long-term impact of emissions from central European cities on regional air quality, *Atmos. Chem. Phys.*, 16, 1331–1352, doi:10.5194/acp-16-1331-2016, 2016a.
- 690 Huszár, P., Belda, M., Karlický, J., Pišoft, P., and Halenka, T.: The regional impact of urban emissions on climate over central Europe: present and future emission perspectives, *Atmos. Chem. Phys.*, 16, 12993–13013, doi:10.5194/acp-16-12993-2016, 2016b.
- Huszar, P., Karlický, J., Belda, M., Halenka, T. and Pisoft, P.: The impact of urban canopy meteorological forcing on summer photochemistry, *Atmos. Environ.*, 176, 209–228, <https://doi.org/10.1016/j.atmosenv.2017.12.037>, 2018a.
- Huszar, P., Belda, M., Karlický, J., Bardachova, T., Halenka, T., and Pisoft, P.: Impact of urban canopy meteorological forcing on aerosol concentrations, *Atmos. Chem. Phys.*, 18, 14059–14078, <https://doi.org/10.5194/acp-18-14059-2018>, 2018b.
- 695 Huszar, P., Karlický, J., Ďoubalová, J., Šindelářová, K., Nováková, T., Belda, M., Halenka, T., Žák, M., and Pišoft, P.: Urban canopy meteorological forcing and its impact on ozone and PM_{2.5}: role of vertical turbulent transport, *Atmos. Chem. Phys.*, 20, 1977–2016, <https://doi.org/10.5194/acp-20-1977-2020>, 2020a.



- Huszar, P., Karlický, J., Ďoubalová, J., Nováková, T., Šindelářová, K., Švábik, F., Belda, M., Halenka, T., and Žák, M.: The impact of urban land-surface on extreme air pollution over central Europe, *Atmos. Chem. Phys.*, 20, 11655–11681, <https://doi.org/10.5194/acp-20-11655-2020>, 2020b.
- Huszar, P., Karlický, J., Marková, J., Nováková, T., Liaskoni, M., and Bartík, L.: The regional impact of urban emissions on air quality in Europe: the role of the urban canopy effects, *Atmos. Chem. Phys.*, 21, 14309–14332, <https://doi.org/10.5194/acp-21-14309-2021>, 2021.
- Im, U., Poupkou, A., Incecik, S., Markakis, K., Kindap, T., Unal, A., Melas, D., Yenigun, O., Topcu, O., Odman, M. T., Tayanc, M., and Guler, M.: The impact of anthropogenic and biogenic emissions on surface ozone concentrations in Istanbul, *Sci. Total Environ.*, 409, 1255–1265, doi:10.1016/j.scitotenv.2010.12.026, 2011a.
- Im, U., Markakis, K., Poupkou, A., Melas, D., Unal, A., Gerasopoulos, E., Daskalakis, N., Kindap, T., and Kanakidou, M.: The impact of temperature changes on summer time ozone and its precursors in the Eastern Mediterranean, *Atmos. Chem. Phys.*, 11, 3847–3864, doi:10.5194/acp-11-3847-2011, 2011b.
- Im, U. and Kanakidou, M.: Impacts of East Mediterranean megacity emissions on air quality, *Atmos. Chem. Phys.*, 12, 6335–6355, doi:10.5194/acp-12-6335-2012, 2012.
- Im, U., Bianconi, R., Solazzo, E., Kioutsioukis, I., Badia, A., Balzarini, A., Baró, R., Bellasio, R., Brunner, D., Chemel, C., Curci, G., Flemming, J., Forkel, R., Giordano, L., Jiménez-Guerrero, P., Hirtl, M., Hodzic, A., Honzak, L., Jorba, O., Knote, C., Kuenen, J. J., Makar, P. A., Manders-Groot, A., Neal, L., Pérez, J. L., Pirovano, G., Pouliot, G., San Jose, R., Savage, N., Schroder, W., Sokhi, R. S., Syrakov, D., Torian, A., Tuccella, P., Werhahn, J., Wolke, R., Yahya, K., Zabkar, R., Zhang, Y., Zhang, J., Hogrefe, C., and Galmarini, S.: Evaluation of operational on-line-coupled regional air quality models over Europe and North America in the context of AQMEII phase 2. 10Part I: Ozone, *Atmos. Environ.*, 115, 404–420, <https://doi.org/10.1016/j.atmosenv.2014.09.042>, 2015.
- IUPAC: Task Group on Atmospheric Chemical Kinetic Data Evaluation, <http://iupac.pole-ether.fr/#>, 2019.
- Jacobson, M. Z., Nghiem, S. V., Sorichetta, A., and Whitney, N.: Ring of impact from the mega-urbanization of Beijing between 2000 and 2009, *J. Geophys. Res.*, 120(12), 5740–5756, <https://doi.org/10.1002/2014JD023008>, 2015.
- Janssen, R. H. H., Tsimpidi, A. P., Karydis, V. A., Pozzer, A., Lelieveld, J., Crippa, M., Prévôt, A. S. H., Ait-Helal, W., Borbon, A., Sauvage, S. and Locoge, N.: Influence of local production and vertical transport on the organic aerosol budget over Paris, *J. Geophys. Res.*, 122(15), 8276–8296, <https://doi.org/10.1002/2016JD026402>, 2017.
- Jiang, X., Wiedinmyer, C., Chen, F., Yang, Z.-L., and Lo, J. C.-F.: Predicted impacts of climate and land use change on surface ozone in the Houston, Texas, area, *J. Geophys. Res.*, 113, D20312, doi:10.1029/2008JD009820, 2008.
- Kang, H., Zhu, B., de Leeuw, G., Yu, B., van der A, R. J., and Lu, W.: Impact of urban heat island on inorganic aerosol in the lower free troposphere: a case study in Hangzhou, China, *Atmos. Chem. Phys. Discuss.* [preprint], <https://doi.org/10.5194/acp-2022-93>, in review, 2022.
- Karlický, J., Huszár, P. and Halenka, T.: Validation of gas phase chemistry in the WRF-Chem model over Europe, *Adv. Sci. Res.*, 14, 181–186, <https://doi.org/10.5194/asr-14-181-2017>, 2017.
- Karlický, J., Huszár, P., Halenka, T., Belda, M., Žák, M., Pišoft, P., and Mikšovský, J.: Multi-model comparison of urban heat island modelling approaches, *Atmos. Chem. Phys.*, 18, 10655–10674, doi:10.5194/acp-18-10655-2018, 2018.
- Karlický, J., Huszár, P., Nováková, T., Belda, M., Švábik, F., Ďoubalová, J., and Halenka, T.: The “urban meteorology island”: a multi-model ensemble analysis, *Atmos. Chem. Phys.*, 20, 15061–15077, <https://doi.org/10.5194/acp-20-15061-2020>, 2020.
- Kesselmeier, J. and Staudt, M.: Biogenic Volatile Organic Compounds (VOC): an overview on emission, physiology and ecology, *J. Atmos. Chem.*, 33, 23–88, 1999.



- Kim, Y, Sartelet, K., Raut, J.-Ch., and Chazette, P.: Influence of an urban canopy model and PBL schemes on vertical mixing for air quality modeling over Greater Paris, *Atmos. Environ.*, 107, 289–306, doi:10.1016/j.atmosenv.2015.02.011, 2015
- Kim, G., Lee, J., Lee, M-I and Kim, D.: Impacts of urbanization on atmospheric circulation and aerosol transport in a coastal environment simulated by the WRF-Chem coupled with urban canopy model, *Atmos. Environ.*, 249, 118253, <https://doi.org/10.1016/j.atmosenv.2021.118253>, 2021.
- 740 Khomenko, S., Cirach, M., Pereira-Barboza, E., Mueller, N., Barrera-Gómez, J., Rojas-Rueda, D., de Hoogh, K., Hoek, G., and Nieuwenhuijsen, M.: Premature mortality due to air pollution in European cities: a health impact assessment, *Lancet Planetary Health*, 3, S2542519620302722, [https://doi.org/10.1016/S2542-5196\(20\)30272-2](https://doi.org/10.1016/S2542-5196(20)30272-2), 2021.
- 745 Kusaka, H., Kondo, K., Kikegawa, Y., and Kimura, F.: A simple single-layer urban canopy model for atmospheric models: Comparison with multi-layer and slab models, *Bound.-Lay. Meteor.*, 101, 329–358, 2001.
- Lawrence, M. G., Butler, T. M., Steinkamp, J., Gurjar, B. R., and Lelieveld, J.: Regional pollution potentials of megacities and other major population centers, *Atmos. Chem. Phys.*, 7, 3969–3987, doi:10.5194/acp-7-3969-2007, 2007.
- Li, Y., Zhang, J., Sailor, D. J., and Ban-Weiss, G. A.: Effects of urbanization on regional meteorology and air quality in Southern California, *Atmos. Chem. Phys.*, 19, 4439–4457, <https://doi.org/10.5194/acp-19-4439-2019>, 2019.
- 750 Liao, J., Wang, T., Wang, X., Xie, M., Jiang, Z., Huang, X. and Zhu, J.: Impacts of different urban canopy schemes in WRF/Chem on regional climate and air quality in Yangtze River Delta, China, *Atmos. Res.*, 145–146, 226–243, <https://doi.org/10.1016/j.atmosres.2014.04.005>, 2014.
- López-Romero, J. M., Montávez, J. P., Jerez, S., Lorente-Plazas, R., Palacios-Peña, L., and Jiménez-Guerrero, P.: Precipitation response to aerosol–radiation and aerosol–cloud interactions in regional climate simulations over Europe, *Atmos. Chem. Phys.*, 21, 415–430, <https://doi.org/10.5194/acp-21-415-2021>, 2021.
- 755 Luecken, D., Yarwood, G., and Hutzell, W.: Multipollutant modeling of ozone, reactive nitrogen and HAPs across the continental US with CMAQ-CB6, *Atmospheric Environment*, 201, 62 – 72, <https://doi.org/https://doi.org/10.1016/j.atmosenv.2018.11.060>, 2019.
- Markakis, K., Valari, M., Perrussel, O., Sanchez, O., and Honore, C.: Climate-forced air-quality modeling at the urban scale: sensitivity to model resolution, emissions and meteorology, *Atmos. Chem. Phys.*, 15, 7703–7723, <https://doi.org/10.5194/acp-15-7703-2015>, 2015.
- 760 Martilli, A., Yves-Alain Roulet, Martin Junier, Frank Kirchner, Mathias W. Rotach, Alain Clappier, On the impact of urban surface exchange parameterisations on air quality simulations: the Athens case, *Atmospheric Environment*, Volume 37, Issue 30, September 2003, Pages 4217–4231, ISSN 1352-2310, [http://dx.doi.org/10.1016/S1352-2310\(03\)00564-8](http://dx.doi.org/10.1016/S1352-2310(03)00564-8), 2003.
- McDonald-Buller, E., Wiedinmyer, C., Kimura, Y. and Allen, D.: Effects of land use data on dry deposition in a regional photochemical model for eastern Texas, *J. Air Waste Manage. Assoc.*, 51, 1211–1218, <https://doi.org/10.1080/10473289.2001.10464340>, 2001.
- 765 Mertens, M., Kerkweg, A., Grewe, V., Jöckel, P., and Sausen, R.: Attributing ozone and its precursors to land transport emissions in Europe and Germany, *Atmos. Chem. Phys.*, 20, 7843–7873, <https://doi.org/10.5194/acp-20-7843-2020>, 2020.
- Miao, Y., Che, H., Zhang, X., and Liu, S.: Integrated impacts of synoptic forcing and aerosol radiative effect on boundary layer and pollution in the Beijing–Tianjin–Hebei region, China, *Atmos. Chem. Phys.*, 20, 5899–5909, <https://doi.org/10.5194/acp-20-5899-2020>, 2020.
- 770 Nenes, A., Pandis, S. N., and Pilinis, C.: ISORROPIA: a new thermodynamic equilibrium model for multiphase multicomponent inorganic aerosols, *Aquat. Geochem.*, 4, 123–152, 1998.
- Oke, T. R.: The energetic basis of the urban heat island, *Q. J. Roy. Meteor. Soc.*, 108, 1–24, <https://doi.org/10.1002/qj.49710845502>, 1982.
- Oke, T., Mills, G., Christen, A., and Voegt, J.: *Urban Climates*, Cambridge University Press, <https://doi.org/10.1017/9781139016476>, 2017.



- Oleson, K. W., Bonan, G. B., Feddema, J., Vertenstein, M., and Grimmond, C. S. B.: An urban parameterization for a global climate model. 775 I. Formulation and evaluation for two cities. *J. Appl. Meteor. Clim.*, 47,1038–1060, 2008.
- Oleson, K.W., Bonan, G.B., Feddema, J., Vertenstein, M., and Kluzek, E.: Technical Description of an Urban Parameterization for the Community Land Model (CLMU), NCAR TECHNICAL NOTE NCAR/TN-480+STR, National Center for Atmospheric Research, Boulder, Co, USA, pp. 61–88, 2010.
- Oleson, K., Lawrence, D. M., Bonan, G. B., Drewniak, B., Huang, M., Koven, C. D., Levis, S., Li, F., Riley, W. J., Subin, Z. M., Swenson, 780 S. C., Thornton, P. E., Bozbiyik, A., Fisher, R., Heald, C. L., Kluzek, E., Lamarque, J.-F., Lawrence, P. J., Leung, L. R., Lipscomb, W., Muszala, S., Ricciuto, D. M., Sacks, W., Sun, Y., Tang, J., and Yang, Z.-L.: Technical Description of version 4.5 of the Community Land Model (CLM), NCAR Technical Note NCAR/TN-503+STR, Boulder, Colorado, 420 pp., 2013.
- Panagi, M., Fleming, Z. L., Monks, P. S., Ashfold, M. J., Wild, O., Hollaway, M., Zhang, Q., Squires, F. A., and Vande Hey, J. D.: Investigating the regional contributions to air pollution in Beijing: a dispersion modelling study using CO as a tracer, *Atmos. Chem. Phys.*, 20, 785 2825–2838, <https://doi.org/10.5194/acp-20-2825-2020>, 2020.
- Park, R. J., Hong, S. K., Kwon, H.-A., Kim, S., Guenther, A., Woo, J.-H., and Loughner, C. P.: An evaluation of ozone dry deposition simulations in East Asia, *Atmos. Chem. Phys.*, 14, 7929–7940, <https://doi.org/10.5194/acp-14-7929-2014>, 2014.
- Passant, N.: Speciation of UK Emissions of Non-methane Volatile Organic Compounds, DEFRA, Oxon, UK, 2002.
- Ren, Y., Zhang, H., Wei, W., Wu, B., Cai, X., and Song, Y.: Effects of turbulence structure and urbanization on the heavy haze pollution 790 process, *Atmos. Chem. Phys.*, 19, 1041–1057, <https://doi.org/10.5194/acp-19-1041-2019>, 2019.
- Ribeiro, F. N. D., Amauri P. de Oliveira, Jacyra Soares, Regina M. de Miranda, Michael Barlage, Fei Chen: Effect of sea breeze propagation on the urban boundary layer of the metropolitan region of Sao Paulo, Brazil, *Atmos. Res.*, 214, 174–188, <https://doi.org/10.1016/j.atmosres.2018.07.015>, 2018.
- Ryu, Y.-H., Baik, J.-J., Kwak, K.-H., Kim, S. and Moon, N.: Impacts of urban land-surface forcing on ozone air quality in the Seoul metropolitan area. *Atmos. Chem. Phys.* 13, 2177–2194. <http://dx.doi.org/10.5194/acp-13-2177-2013>, 2013. 795
- Sarrat, C., Lemonsu, A., Masson, V., and Guedalia, D.: Impact of urban heat island on regional atmospheric pollution, *Atmos. Environ.*, 40, 1743–1758, 2006.
- Seinfeld, J. H. and Pandis, S. N.: *Atmospheric Chemistry and Physics: From Air Pollution to Climate Change*, J. Wiley, New York, 1998.
- Simmons, A. J., Willett, K. M., Jones, P. D., Thorne, P. W., and Dee, D. P.: Low-frequency variations in surface atmospheric humidity, 800 temperature and precipitation: inferences from reanalyses and monthly gridded observational datasets, *J. Geophys. Res.*, 115, D01110, doi:10.1029/2009JD012442, 2010.
- Sindelarova, K., Granier, C., Bouarar, I., Guenther, A., Tilmes, S., Stavrou, T., Müller, J.-F., Kuhn, U., Stefani, P., and Knorr, W.: Global data set of biogenic VOC emissions calculated by the MEGAN model over the last 30 years, *Atmos. Chem. Phys.*, 14, 9317–9341, <https://doi.org/10.5194/acp-14-9317-2014>, 2014.
- 805 Sindelarova, K., Markova, J., Simpson, D., Huszar, P., Karlicky, J., Darras, S., and Granier, C.: High-resolution biogenic global emission inventory for the time period 2000–2019 for air quality modelling, *Earth Syst. Sci. Data*, 14, 251–270, <https://doi.org/10.5194/essd-14-251-2022>, 2022.
- Situ, S., Guenther, A., Wang, X., Jiang, X., Turnipseed, A., Wu, Z., Bai, J., and Wang, X.: Impacts of seasonal and regional variability in biogenic VOC emissions on surface ozone in the Pearl River delta region, China, *Atmos. Chem. Phys.*, 13, 11803–11817, 810 <https://doi.org/10.5194/acp-13-11803-2013>, 2013.



- Skamarock, W. C., J. B. Klemp, J. Dudhia, D. O. Gill, Z. Liu, J. Berner, W. Wang, J. G. Powers, M. G. Duda, D. M. Barker, and X.-Y. Huang: A Description of the Advanced Research WRF Version 4. NCAR Tech. Note NCAR/TN-556+STR, 145 pp. doi:10.5065/1dfh-6p97, 2019.
- Skyllakou, K., Murphy, B. N., Megaritis, A. G., Fountoukis, C., and Pandis, S. N.: Contributions of local and regional sources to fine PM in the megacity of Paris, *Atmos. Chem. Phys.*, 14, 2343–2352, doi:10.5194/acp-14-2343-2014, 2014.
- 815 Slater, J., Coe, H., McFiggans, G., Tonttila, J., and Romakkaniemi, S.: The effect of BC on aerosol–boundary layer feedback: potential implications for urban pollution episodes, *Atmos. Chem. Phys.*, 22, 2937–2953, <https://doi.org/10.5194/acp-22-2937-2022>, 2022.
- Sokhi, R. S., Moussiopoulos, N., Baklanov, A., Bartzis, J., Coll, I., Finardi, S., Friedrich, R., Geels, C., Grönholm, T., Halenka, T., Ketzler, M., Maragkidou, A., Matthias, V., Moldanova, J., Ntziachristos, L., Schäfer, K., Suppan, P., Tsegas, G., Carmichael, G., Franco, V., Hanna, S., Jalkanen, J.-P., Velders, G. J. M., and Kukkonen, J.: Advances in air quality research – current and emerging challenges, *Atmos. Chem. Phys.*, 22, 4615–4703, <https://doi.org/10.5194/acp-22-4615-2022>, 2022.
- 820 Song, J., Webb, A., Parmenter, B. Allen, D. T. and McDonald-Buller, E.: *Environmental Sci. Tech.*, 42(19), 7294-7300 DOI: 10.1021/es800645j, 2008.
- Stock, Z. S., Russo, M. R., Butler, T. M., Archibald, A. T., Lawrence, M. G., Telford, P. J., Abraham, N. L., and Pyle, J. A.: Modelling the impact of megacities on local, regional and global tropospheric ozone and the deposition of nitrogen species, *Atmos. Chem. Phys.*, 13, 12215–12231, <https://doi.org/10.5194/acp-13-12215-2013>, 2013.
- 825 Strader, R. Lurmann, F. and Pandis, S. N.: Evaluation of secondary organic aerosol formation in winter, *Atmos. Environ.*, 33., 4849-4863, 1999.
- Struzewska, J. and Kaminski, J. W.: Impact of urban parameterization on high resolution air quality forecast with the GEM – AQ model, *Atmos. Chem. Phys.*, 12, 10387–10404, <https://doi.org/10.5194/acp-12-10387-2012>, 2012.
- 830 Tagaris, E., Sotiropoulou, R. E. P., Gounaris, N., Andronopoulos, S., and Vlachogiannis, D.: Impact of biogenic emissions on ozone and fine particles over Europe: Comparing effects of temperature increase and a potential anthropogenic NO_x emissions abatement strategy, *Atmos. Environ.*, 98, 214–223, <https://doi.org/10.1016/j.atmosenv.2014.08.056>, 2014.
- Tao, Z., Santanello, J.A., Chin, M., Zhou, S., Tan, Q., Kemp, E.M., Peters-Lidard, C.D.: Effect of land cover on atmospheric processes and air quality over the continental United States - a NASA Unified WRF (NU-WRF) model study. *Atmos. Chem. Phys.* 13, 6207–6226. <http://dx.doi.org/10.5194/acp-13-6207-2013>.
- 835 Tao, W., Liu, J., Ban-Weiss, G. A., Hauglustaine, D. A., Zhang, L., Zhang, Q., Cheng, Y., Yu, Y., and Tao, S.: Effects of urban land expansion on the regional meteorology and air quality of eastern China, *Atmos. Chem. Phys.*, 15, 8597–8614, <https://doi.org/10.5194/acp-15-8597-2015>, 2015.
- Thunis, P., Clappier, A., de Meij, A., Pisoni, E., Bessagnet, B., and Tarrason, L.: Why is the city’s responsibility for its air pollution often underestimated? A focus on PM_{2.5}, *Atmos. Chem. Phys.*, 21, 18195–18212, <https://doi.org/10.5194/acp-21-18195-2021>, 2021.
- 840 Tie, X., Brasseur, G., and Ying, Z.: Impact of model resolution on chemical ozone formation in Mexico City: application of the WRF-Chem model, *Atmos. Chem. Phys.*, 10, 8983-8995, <https://doi.org/10.5194/acp-10-8983-2010>, 2010.
- Tie, X., Geng, F., Guenther, A., Cao, J., Greenberg, J., Zhang, R., Apel, E., Li, G., Weinheimer, A., Chen, J., and Cai, C.: Megacity impacts on regional ozone formation: observations and WRF-Chem modeling for the MIRAGE-Shanghai field campaign, *Atmos. Chem. Phys.*, 13, 5655–5669, <https://doi.org/10.5194/acp-13-5655-2013>, 2013.
- 845 Tiedtke, M.: A Comprehensive Mass Flux Scheme for Cumulus Parameterization in Large-Scale Models, *Mon. Weather Rev.*, 117, 1779-1800, [https://doi.org/10.1175/1520-0493\(1989\)117](https://doi.org/10.1175/1520-0493(1989)117), 1989.



- Timothy, M. and Lawrence, M. G.: The influence of megacities on global atmospheric chemistry: a modeling study, *Environ. Chem.*, 6, 219–225, doi:10.1071/EN08110, 2009.
- 850 Toma, S., Bertman, S., Groff, C., Xiong, F., Shepson, P. B., Romer, P., Duffey, K., Wooldridge, P., Cohen, R., Baumann, K., Edgerton, E., Koss, A. R., de Gouw, J., Goldstein, A., Hu, W., and Jimenez, J. L.: Importance of biogenic volatile organic compounds to acyl peroxy nitrates (APN) production in the southeastern US during SOAS 2013, *Atmos. Chem. Phys.*, 19, 1867–1880, <https://doi.org/10.5194/acp-19-1867-2019>, 2019.
- Tuccella, P., Curci, G., Visconti, G., Bessagnet, B., Menut, L., and Park, R. J.: Modeling of gas and aerosol with WRF/Chem over Europe: Evaluation and sensitivity study, *J. Geophys. Res.*, 117, D03303, <https://doi.org/10.1029/2011JD016302>, 2012.
- 855 Ulpiani, G.: On the linkage between urban heat island and urban pollution island: Three-decade literature review towards a conceptual framework, *Sci. Total Environ.*, 751, 141727, <https://doi.org/10.1016/j.scitotenv.2020.141727>, 2021.
- UN: The 2018 Revision of the World Urbanization Prospects, Population Division of the United Nations Department of Economic and Social Affairs (UN DESA), New York, <https://www.un.org/development/desa/publications/2018-revision-of-world-urbanization-prospects.html>.
- 860 2018.
- Wang, X. M., Lin, W. S., Yang, L. M., Deng, R. R., and Lin, H.: A numerical study of influences of urban land-use change on ozone distribution over the Pearl River Delta region, China, *Tellus*, 59B, 633–641, 2007.
- Wang, X., Chen, F., Wu, Z., Zhang, M., Tewari, M., Guenther, A., and Wiedinmyer, C.: Impacts of weather conditions modified by urban expansion on surface ozone: Comparison between the Pearl River Delta and Yangtze River Delta regions, *Adv. Atmos. Sci.*, 26, 962–972,
- 865 2009.
- Wang, Y., Ma, Y.-F., Muñoz-Esparza, D., Li, C. W. Y., Barth, M., Wang, T., and Brasseur, G. P.: The impact of inhomogeneous emissions and topography on ozone photochemistry in the vicinity of Hong Kong Island, *Atmos. Chem. Phys.*, 21, 3531–3553, <https://doi.org/10.5194/acp-21-3531-2021>, 2021.
- Wang, M., Tang, G., Liu, Y., Ma, M., Yu, M., Hu, B., Zhang, Y., Wang, Y. and Wang, Y.: The difference in the boundary
- 870 layer height between urban and suburban areas in Beijing and its implications for air pollution, *Atmos. Environ.*, 260, 118552, <https://doi.org/10.1016/j.atmosenv.2021.118552>, 2021.
- Wang, J., Xing, J., Wang, S., Mathur, R., Wang, J., Zhang, Y., Liu, C., Pleim, J., Ding, D., Chang, X., Jiang, J., Zhao, P., Sahu, S. K., Jin, Y., Wong, D. C., and Hao, J.: The pathway of impacts of aerosol direct effects on secondary inorganic aerosol formation, *Atmos. Chem. Phys.*, 22, 5147–5156, <https://doi.org/10.5194/acp-22-5147-2022>, 2022.
- 875 Xie, M., Zhu, K., Wang, T., Feng, W., Gao, D., Li, M., Li, S., Zhuang, B., Han, Y., Chen, P., and Liao, J.: Changes in regional meteorology induced by anthropogenic heat and their impacts on air quality in South China, *Atmos. Chem. Phys.*, 16, 15011–15031, <https://doi.org/10.5194/acp-16-15011-2016>, 2016a.
- Xie, M., Liao, J., Wang, T., Zhu, K., Zhuang, B., Han, Y., Li, M., and Li, S.: Modeling of the anthropogenic heat flux and its effect on regional meteorology and air quality over the Yangtze River Delta region, China, *Atmos. Chem. Phys.*, 16, 6071–6089, <https://doi.org/10.5194/acp-16-6071-2016>, 2016b.
- 880 Xue, L. K., Wang, T., Gao, J., Ding, A. J., Zhou, X. H., Blake, D. R., Wang, X. F., Saunders, S. M., Fan, S. J., Zuo, H. C., Zhang, Q. Z., and Wang, W. X.: Ground-level ozone in four Chinese cities: precursors, regional transport and heterogeneous processes, *Atmos. Chem. Phys.*, 14, 13175–13188, doi:10.5194/acp-14-13175-2014, 2014.
- Yienger, J. J. and Levy, H.: Empirical model of global soil-biogenic NO_x emissions, *J. Geophys. Res. Atmos.*, 100 (D6), 11447–11464, <https://doi.org/10.1029/95JD00370>, 1995.
- 885



- Yim, S. H. L., Wang, M., Gu, Y., Yang, Y., Dong, G., and Li, Q.: Effect of urbanization on ozone and resultant health effects in the Pearl River Delta region of China, *J. Geophys. Res. Atmos.*, 124, 11568–11579, <https://doi.org/10.1029/2019JD030562>, 2019.
- Yu, M., Tang, G., Yang, Y., Li, Q., Wang, Y., Miao, S., Zhang, Y., and Wang, Y.: The interaction between urbanization and aerosols during a typical winter haze event in Beijing, *Atmos. Chem. Phys.*, 20, 9855–9870, <https://doi.org/10.5194/acp-20-9855-2020>, 2020.
- 890 Zanis, P., Katragkou, E., Tegoulas, I., Poupkou, A., Melas, D., Huszar, P. and Giorgi, F.: Evaluation of near surface ozone in air quality simulations forced by a regional climate model over Europe for the period 1991–2000, *Atmos. Environ.*, 45, 6489–6500, <https://doi.org/10.1016/j.atmosenv.2011.09.001>, 2011.
- Zha, J., Zhao, D., Wu, J. and Zhang, P.: Numerical simulation of the effects of land use and cover change on the near-surface wind speed over Eastern China, *Clim. Dyn.*, <https://doi.org/10.1007/s00382-019-04737-w>, 2019.
- 895 Zhang, L., Brook, J. R., and Vet, R.: A revised parameterization for gaseous dry deposition in air-quality models, *Atmos. Chem. Phys.*, 3, 2067–2082, <https://doi.org/10.5194/acp-3-2067-2003>, 2003.
- Zhao, L., Lee, X., and Schultz, N. M.: A wedge strategy for mitigation of urban warming in future climate scenarios, *Atmos. Chem. Phys.*, 17, 9067–9080, <https://doi.org/10.5194/acp-17-9067-2017>, 2017.
- Zhong, S., Qian, Y., Sarangi, C., Zhao, C., Leung, R., Wang, H., et al.: Urbanization effect on winter haze in the Yangtze River Delta region
900 of China, *Geophys. Res. Letters*, 45., <https://doi.org/10.1029/2018GL077239>, 2018.
- Zhou, S., Yang, J., Wang, W.-C., Zhao, C., Gong, D., and Shi, P.: An observational study of the effects of aerosols on diurnal variation of heavy rainfall and associated clouds over Beijing–Tianjin–Hebei, *Atmos. Chem. Phys.*, 20, 5211–5229, <https://doi.org/10.5194/acp-20-5211-2020>, 2020.
- Zhu, B., Kang, H., Zhu, T., Su, J., Hou, X., and Gao, J. Impact of Shanghai urban land surface forcing on downstream city ozone chemistry,
905 *J. Geophys. Res.*, 120(9) 4340–4351, 2015.
- Zhu, K., Xie, M., Wang, T., Cai, J., Li, S., and Feng, W.: A modeling study on the effect of urban land surface forcing to regional meteorology and air quality over South China, *Atmos. Environ.*, 152, 389–404, <http://dx.doi.org/10.1016/j.atmosenv.2016.12.053>, 2017.



Table 1. The list of RCM simulations performed.

Regional Climate Model (RCM) runs		
Model	Urbanization ^a	Resolution[km]
RegCM	Urban	9/3/1 ^b
RegCM	Nourban	9/3/1
WRF	Urban	9
WRF	Nourban	9

^aInformation whether urban land-surface was considered.

^bSimulation performed in a nested way at 9, 3 and 1 km horizontal resolution.

Table 2. The list of CTM simulations performed with the information of the effects considered. The "Driving meteorology" and "BVOC (meteorology)" columns correspond to the "Urbanization" information from Tab. 1 above.

Regional Chemistry Transport Model (CTM) runs						
	Experiment	Driving meteorology	Urban emissions	Landuse (deposition)	BVOC (landuse)	BVOC (meteorology)
1	ENNrN (Reference)	Nourban	No	Rural	Rural	Nourban ^a
2	ENYrrN	Nourban	Yes	Rural	Rural	Nourban
3	ENYurN	Nourban	Yes	Urban	Rural	Nourban
4	ENYuuN	Nourban	Yes	Urban	Urban	Nourban
5	ENYuuU	Nourban	Yes	Urban	Urban	Urban
6	EUYuuU	Urban	Yes	Urban	Urban	Urban

^ainformation whether the meteorology driving the MEGAN model accounted for the UCMF

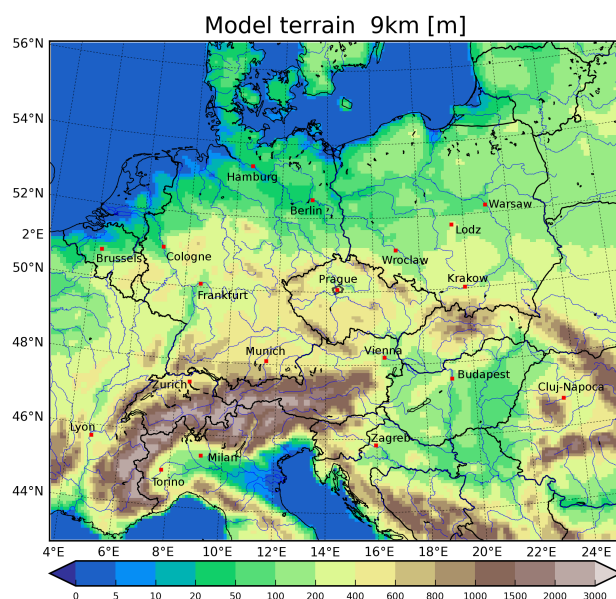


Figure 1. The resolved model terrain in meters for the 9 km x 9 km domain and the cities analyzed in the study (red squares).

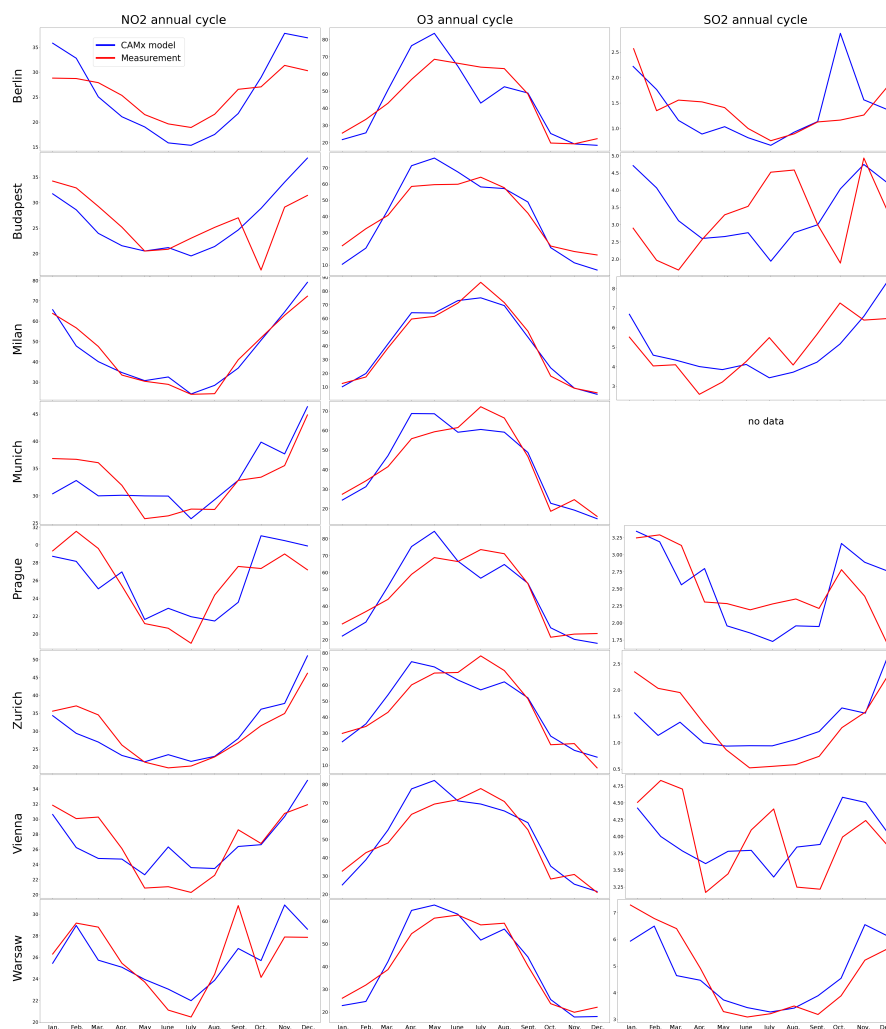


Figure 2. Comparison of modelled (blue) and measured (red; AirBase data) urban and suburban average monthly concentrations of NO_2 (left), O_3 (middle) and SO_2 (right) for eight different cities selected from the total 19 considered in the study, namely Berlin, Budapest, Milan, Munich, Prague, Zurich, Vienna and Warsaw. Units in $\mu\text{g m}^{-3}$. Data are averaged across all available urban and suburban background stations within the chosen city. No data for SO_2 in Munich as no corresponding measuring station was available.

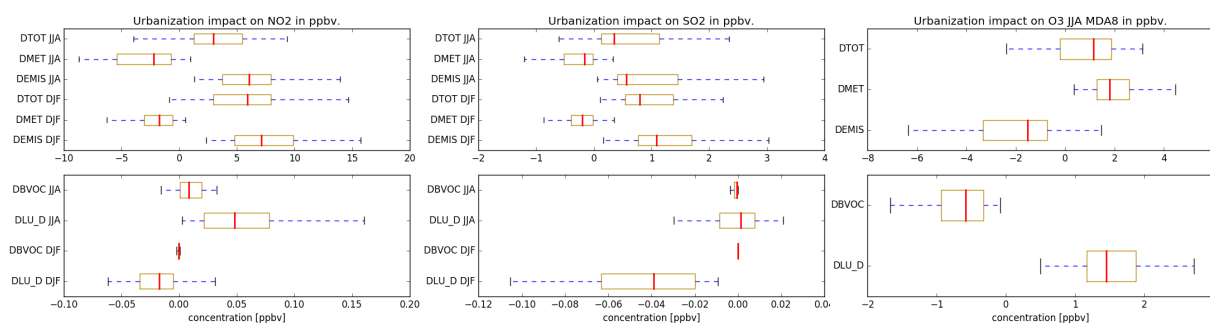


Figure 3. The 2015–2016 DJF and JJA averaged impact of each component of the rural–urban transformation including the total impact averaged over all chosen city for NO₂, SO₂ and O₃ in ppbv. In case of ozone, only the summer averaged MDA8 (maximum daily 8-hour average) is shown. The boxplots show the 25% to 75% quantiles including the minimum and maximum value. The red line showing the median. Values are taken from model grid-cell that covers the city center. The upper sub-figures show the two main impacts including the total impact (“DEMIS“, “DMET“ and “DTOT“) while the lower one the minor contributors (“DLU_D“ and “DBVOC“)

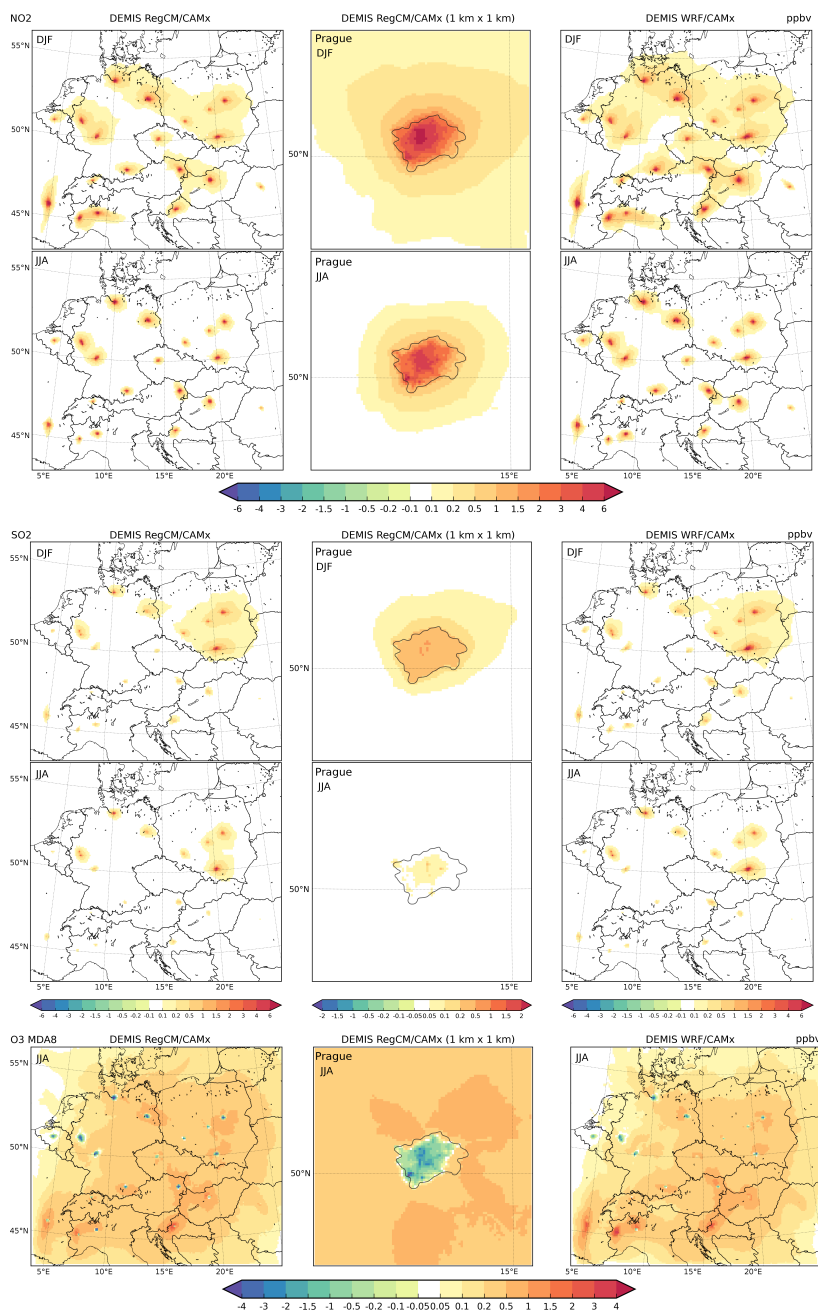


Figure 4. The spatial distribution of the 2015-2016 average emission impact "DEMIS" for NO₂ DJF and JJA (1st and 2nd row), SO₂ DJF and JJA (3rd and 4th row) and JJA MDA8 O₃ (5th row). Columns represent the results from the 9 km RegCM/CAMx, the 1 km RegCM/CAMx (detail of Prague) and the 9 km WRF/CAMx simulations. Units in ppbv.

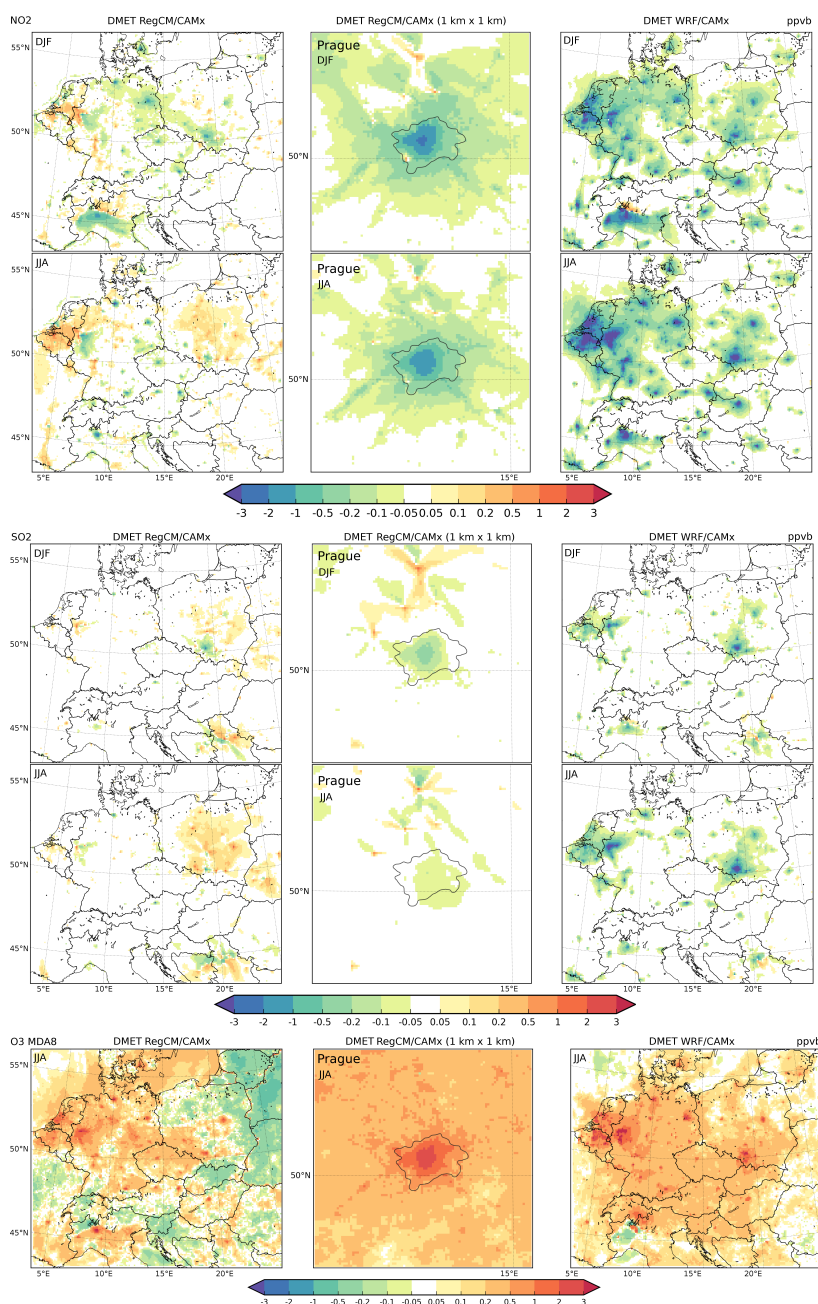


Figure 5. The spatial distribution of the 2015-2016 average impact of the urban canopy meteorological forcing (UCMF) "DMET" on NO_2 DJF and JJA (1st and 2nd row), SO_2 DJF and JJA (3rd and 4th row) and JJA MDA8 O_3 (5th row). Columns represent the results from the 9 km RegCM/CAMx, the 1 km RegCM/CAMx (detail of Prague) and the 9 km WRF/CAMx simulations. Units in ppbv.

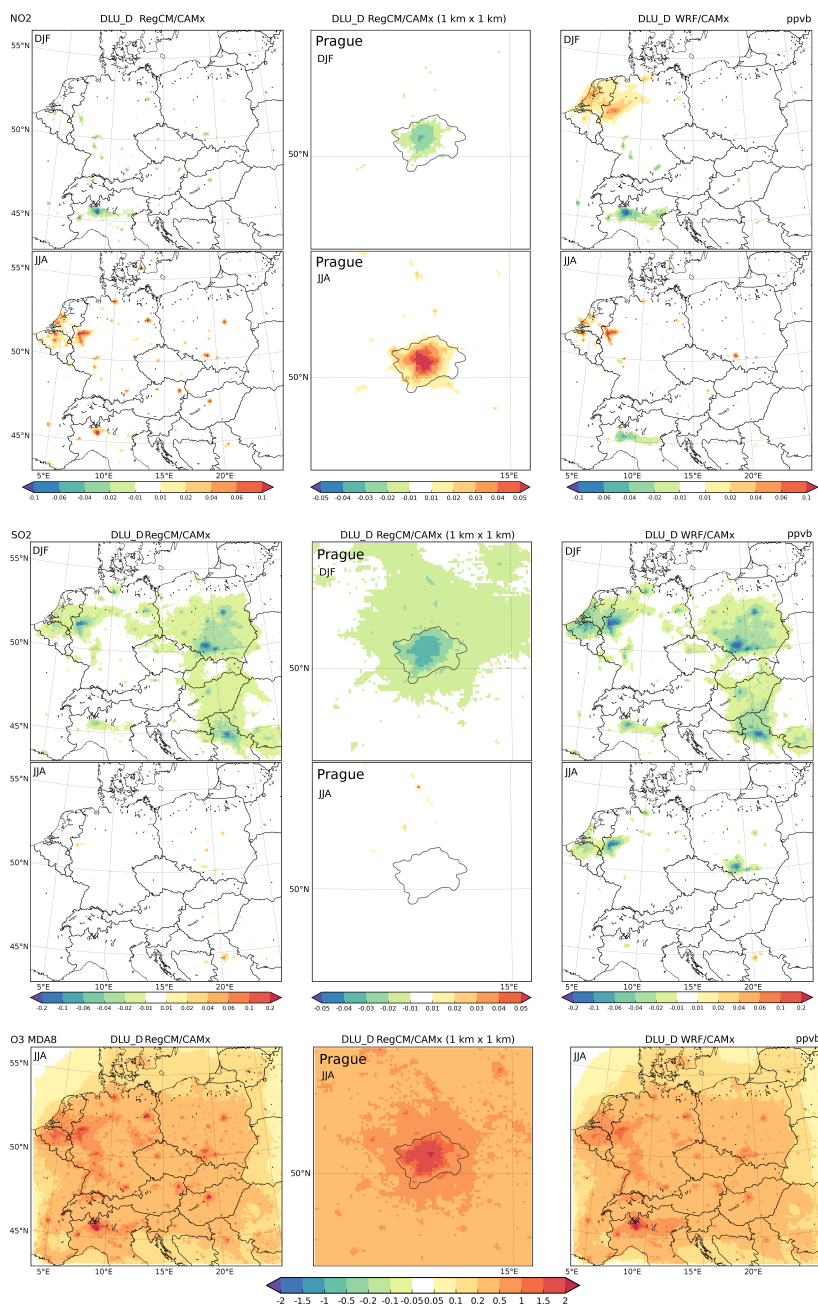


Figure 6. The spatial distribution of the 2015-20216 average impact of the urban land-cover via dry-deposition modifications (“DLU_D”) on NO₂ DJF and JJA (1st and 2nd row), SO₂ DJF and JJA (3rd and 4th row) and JJA MDA8 O₃ (5th row). Columns represent the results from the 9 km RegCM/CAMx, the 1 km RegCM/CAMx (detail of Prague) and the 9 km WRF/CAMx simulations. Units in ppbv.

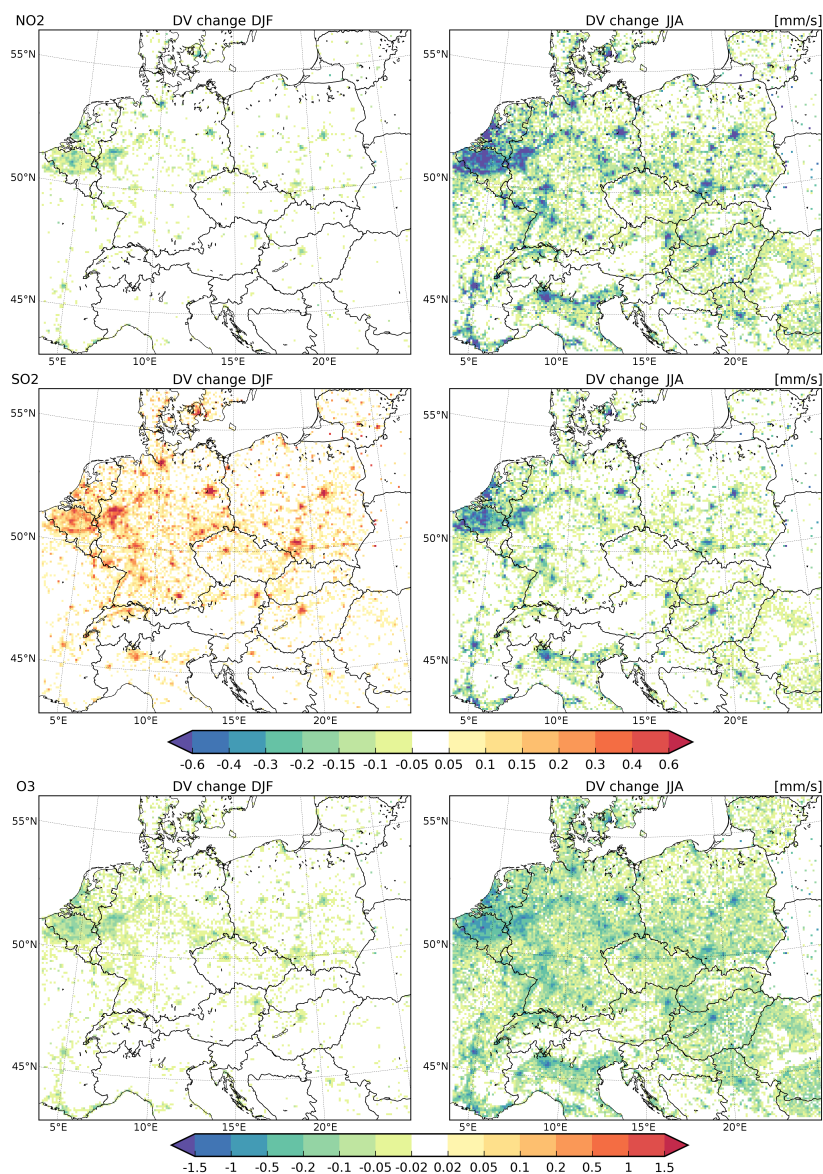


Figure 7. The spatial distribution of the 2015-2016 average impact of the urban land-cover on deposition velocities of NO₂ (1st row), SO₂ (2nd row) and O₃ (3rd row) for DJF (left) and JJA (right) in mm.s⁻¹ for the RegCM driven 9 km CAMx simulations.

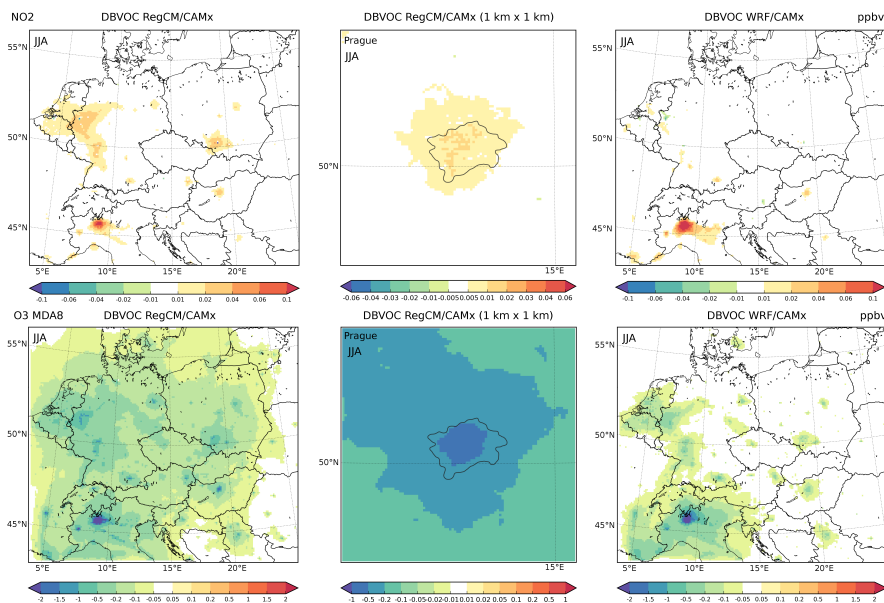


Figure 8. The spatial distribution of the 2015-2016 average impact of the urbanization via modifications of BVOC emissions (“DBVOC”) on JJA NO₂ (upper row) and MDA8 O₃ (lower row). Columns represent the results from the 9 km RegCM/CAMx, the 1 km RegCM/CAMx (detail of Prague) and the 9 km WRF/CAMx simulations. Units in ppbv.

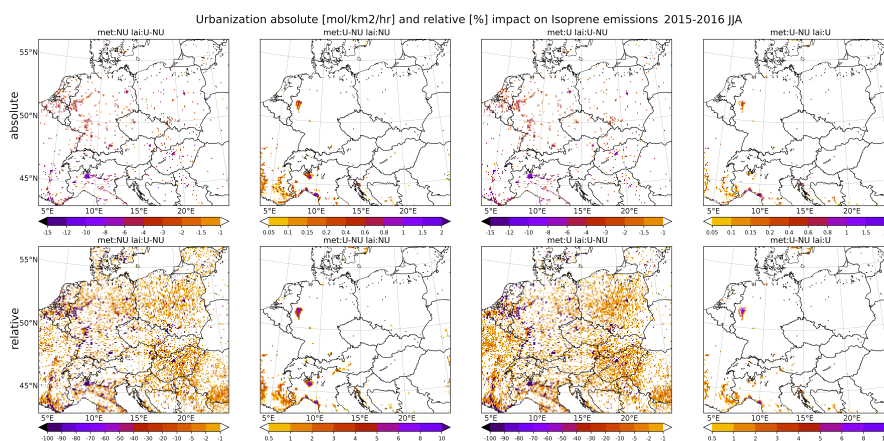


Figure 9. The absolute (upper row; units mol.km⁻².hr⁻¹) and relative change (lower row; units in %) of 2015-2016 JJA averaged isoprene (ISOP) emissions decomposed into the part caused by reduced vegetation (via leaf-area-index; “DBVOC_L”) and the part caused by modified meteorology (“DBVOC_M”). The 1st and 3rd column show the change due to “DBVOC_L” taking the rural (NU) and urban (U) meteorological conditions as a reference, respectively. In the 2nd and 4th columns, the changes due to urban meteorological effects (UCMF) are shown (“DBVOC_M”) taking the rural (NU) and urban (U) vegetation as a reference, respectively.

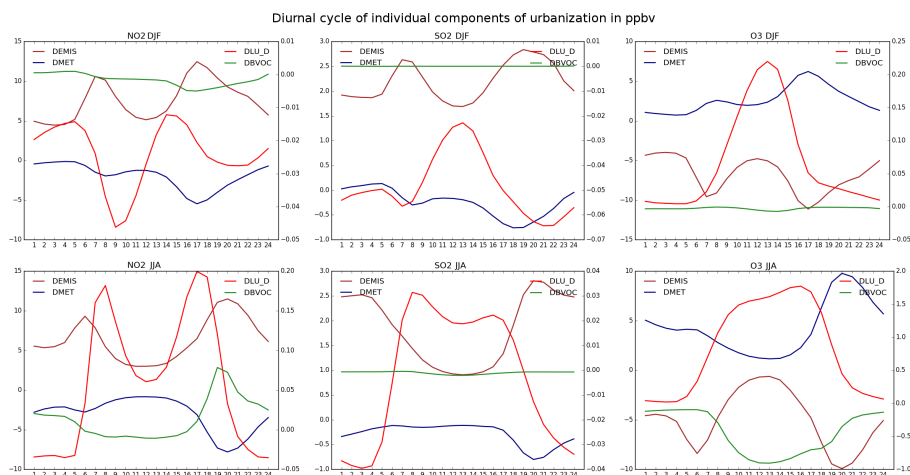


Figure 10. The 2015-2016 average diurnal cycle of the individual components of RUT for NO₂ (left), SO₂ (middle) and O₃ (right) as DJF (upper row) and JJA (bottom row) average. The brown and blue lines stand for the two stronger contributors ("DEMIS" and "DMET", left y-axis), while red and green stand for minor contributors "DLU_D" and "DBVOC" (right y-axis). Units in ppbv. Times in UTC (i.e. the local time is +2 hours in JJA and +1 hours in DJF).

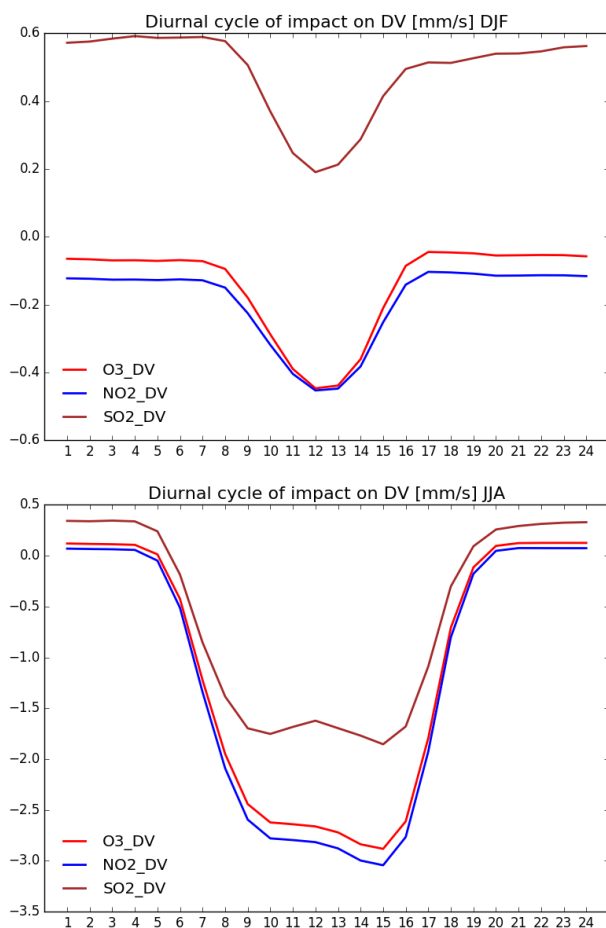


Figure 11. The diurnal cycle of the impact of urbanization on deposition velocities (DV) for 2015-2016 DJF (up) and JJA (bottom) for NO₂ (blue), SO₂ (brown) and O₃ (red) in mm.h⁻¹.